

Research



Cite this article: Breunung T, Haller G. 2018

Explicit backbone curves from spectral submanifolds of forced-damped nonlinear mechanical systems. *Proc. R. Soc. A* **474**: 20180083.

<http://dx.doi.org/10.1098/rspa.2018.0083>

Received: 7 February 2018

Accepted: 12 April 2018

Subject Areas:

mechanical engineering, structural engineering, applied mathematics

Keywords:

backbone curves, nonlinear dynamics, nonlinear oscillations, spectral submanifolds, non-autonomous systems

Author for correspondence:

George Haller

e-mail: georgehaller@ethz.ch

Electronic supplementary material is available online at <https://dx.doi.org/10.6084/m9.figshare.c.4084508>.

Explicit backbone curves from spectral submanifolds of forced-damped nonlinear mechanical systems

Thomas Breunung and George Haller

Institute for Mechanical Systems, ETH Zürich, Leonardstrasse 21, 8092 Zürich, Switzerland

TB, 0000-0001-7885-2201

Spectral submanifolds (SSMs) have recently been shown to provide exact and unique reduced-order models for nonlinear unforced mechanical vibrations. Here, we extend these results to periodically or quasi-periodically forced mechanical systems, obtaining analytic expressions for forced responses and backbone curves on modal (i.e. two dimensional) time-dependent SSMs. A judicious choice of the parametrization of these SSMs allows us to simplify the reduced dynamics considerably. We demonstrate our analytical formulae on three numerical examples and compare them to results obtained from available normal-form methods.

1. Introduction

In drawing conclusions about a nonlinear mechanical system, an engineering analyst usually faces the challenge of high dimensionality and complex dynamic equations. To reduce simulation time and deduce general statements, it is desirable to reduce the dimension of the system and simplify the resulting reduced equations of motion.

For linear systems, decomposition into normal modes is a powerful tool to derive reduced-order models. While the lack of the superposition principle makes such a decomposition impossible for nonlinear systems, various definitions of nonlinear normal modes (NNMs) are also available in the literature (cf. [1–3]). Specifically, Rosenberg [1] defines a NNM as a synchronous periodic orbit of a conservative system. Later, Shaw & Pierre [2] extended this definition to dissipative systems, by viewing a NNM as an invariant manifold tangent to a modal subspace of an equilibrium point. Sought,

in practice, via a Taylor expansion, these manifolds serve as nonlinear continuations of the invariant modal subspaces spanned by the eigenvectors of the linearized system. Owing to their invariance, these manifolds are natural candidates for model order reduction.

While there are generally infinitely many Shaw-Pierre-type surfaces for each modal subspace (cf. [4]), Haller & Ponsioen [3] have shown that, under appropriate non-resonance conditions, there is a unique smoothest one, which they called a spectral submanifold (SSM). When the underlying modal subspace is the one with the slowest decay, the dynamics on its corresponding SSM serves as the optimal, mathematically exact reduced-order model for the system dynamics (see [3]). Applications of this model reduction approach appear in Jain *et al.* [5] and Szalai *et al.* [6]. Ponsioen *et al.* [7] provide an automated computation package for two-dimensional SSMs of a general autonomous, nonlinear mechanical system.

While most of the above work focuses on unforced (autonomous) mechanical systems, here we explore further the utility of SSMs for forced dissipative nonlinear mechanical systems. For this class of systems, the existence, uniqueness and regularity of SSMs have been clarified by Haller & Ponsioen [3], relying on the more abstract invariant manifold results of Haro & de la Lave [8]. In this context, a NNM is defined as the continuation of the trivial hyperbolic fixed point of the time-independent system under the addition of a small time-dependent forcing with a finite number of frequencies. Depending on the frequency content of the time-varying terms, this continuation is a periodic or quasi-periodic orbit (cf. [3]). The SSM will be a time-dependent surface with the same frequency basis. This SSM is then tangent to the NNM along directions associated with a spectral subspace of the linearization.

The first attempt to construct such a non-autonomous SSM can be found in Jiang *et al.* [9], who formally reduce an externally forced, dissipative mechanical system to a two-dimensional time-varying invariant manifold. While their results are promising even for high-amplitude oscillations, they are only able to carry out the reduction numerically for fixed parameter values, aided by a Galerkin projection. Therefore, their study is limited to specific examples and symbolic equations from which general conclusions about the forced response could be derived are not obtained. Furthermore, the uniqueness, existence and smoothness of their assumed invariant manifold remains unclear from their procedure.

Extending this approach to systems with time-periodic coefficients in their linear part, Sinha *et al.* [10] and Gabale & Sinha [11] expand the assumed invariant manifold in a multivariate Taylor-Fourier series, obtaining the unknown coefficients from the invariance of the manifold. With unclear uniqueness, existence and smoothness properties of the manifold, however, the series expansion remains unjustified. Furthermore, the approach does not yield generally applicable closed formulae and hence numerical integration is required to analyse the reduced model.

A generally applicable procedure for the simplification of the (formally) reduced dynamics is the method of normal forms (cf. e.g. [12]). The method applies a series of smooth transformations to obtain a Taylor series of the original dynamical equations, which contain only the terms essential for the dynamics. Jezequel & Lamarque [13] demonstrate the potential of normal forms for mechanical vibrations after the system is transformed to first-order phase-space form. Neild & Wagg [14] give an alternative formulation of the normal form procedure that is directly applicable to second-order mechanical systems. As all state variables are transformed, the resulting dynamics have the same dimensionality as the original system and no model-order reduction is achieved. Furthermore, both of these normal form approaches start from conservative systems and treat damping as a small bifurcation parameter. Therefore, the unfolding from the conservative limit has to be discussed for every damping type separately.

Touzé & Amabili [15] seek to unite normal form theory with model-order reduction for the first time. After a normal form transformation, they restrict their calculations to heuristically chosen submanifolds. As pointed out by the authors, a strict time-varying normal form is not computed. Instead, the forcing is inserted directly into the normal form. This represents phenomenological forcing aligned with a curvilinear coordinates, rather than a specific physical forcing applied to the system.

Owing to the essential nonlinear relationship between forcing and response amplitude of nonlinear systems, a single response curve for a given forcing is meaningless for different forcing amplitudes. To summarize responses obtained from different forcing amplitudes, one may choose to collect distinguished points of various response curves in the same diagram. For instance, Nayfeh & Mook [16] and Cveticanin *et al.* [17] call the curve formed by the loci of the maximal response amplitude the backbone curve. Cveticanin *et al.* [17] further trace fold points of the forced response and relate them to the maximum amplitude. Both Nayfeh & Mook [16] and Cveticanin *et al.* [17], however, compute the backbone curves only for low-dimensional specific examples. Furthermore, Peeters *et al.* [18] trace the frequencies at which the forced response is 90° out of phase to the forcing.

An alternative given by Klotter [19] and continued by Rosenberg & Atkinson [20] is the definition of the backbone curve as the frequency–amplitude relationship of a periodic solution family of the conservative unforced limit of the system. Additional arguments are necessary to justify the relevance of these curves for forced-damped vibrations. Hill *et al.* [21,22], Kerschen *et al.* [23] and Peeters *et al.* [18] observe that along each NNM (i.e. periodic orbit) of the conservative limit, weak viscous damping can be cancelled by an appropriately chosen external periodic forcing. Under such forcing, the conservative set of NNMs will form the backbone curves. For a general damped and forced nonlinear system, however, the relevance of periodic orbits of the conservative limit for the forced response is not well understood. Recently, Hill *et al.* [22] observed numerically that major parts of such NNMs are non-robust and therefore irrelevant for the forced response. They propose a robustness measure to assess the relevance of the conservative NNMs for the forced response. Kerschen *et al.* [23] and Peeters *et al.* [18] mention specific examples in which the forced response of an almost conservative system will be close to the periodic orbits of the conservative system. As the backbone curve is obtained for the unforced conservative limit in these examples, another method is needed to actually calculate the maximum amplitude for a given forcing. Hill *et al.* [21] present an energy transfer-based method for this purpose. They also give, however, a counterexample in which the conservative backbone curve has no relevance for the forced response.

Parallel to theoretical considerations, backbone curves have been approximated in experiments through the *force appropriation method*. In this method, the nonlinear system is forced with a harmonic forcing such that the response has a 90° phase lag in a modal degree of freedom. While this force appropriation procedure is plausible for linear viscous damping (or nonlinear damping that is an odd function of the velocities), the approach has remained unjustified for general, nonlinear damping (cf. [18]).

An experimental alternative to the force appropriation is the *resonance decay* method, in which the system is forced, such that its response is close to an envisaged invariant surface of the conservative limit. Then the forcing is turned off and the instantaneous amplitude–frequency relationship is identified by signal processing. Peeters *et al.* [18], however, relate this curve, which is essentially a feature of the damped system, to the orbits of the conservative system only phenomenologically.

We also note that force appropriation and the resonance decay aim to reconstruct NNMs of the conservative limit. The set formed by these orbits is expected to deviate from the forced response of the actual dissipative system for larger amplitudes and larger damping. As a recent development, Szalai *et al.* [6] compute the backbone curves from the frequency–amplitude relationship of decaying vibrations on SSMs reconstructed from measured data. A connection with the backbone curve obtained from the forced response, however, is not immediate.

In summary, available approaches to compute forced response via model reduction for nonlinear mechanical systems suffer either from heuristic steps or omissions in the reduction procedure, or from an unclear relationship between backbone-curve definitions different from the one relevant for forced-damped vibrations in a practical setting. In this work, we seek to eliminate these shortcomings simultaneously. First, we employ a mathematically justified reduction process to time-dependent SSMs in the presence of general damping and forcing. Second, with universal, system-independent formulae for the dynamics on the SSM at hand,

we derive explicit, leading-order approximations to the actually observed backbone curve of the time-dependent, dissipative response. We show how all this can be achieved without the use of extensive numerics (such as numerical continuation or numerical time integration) or extensive numerical experimentation (force appropriation and resonance decay).

Our results are based on a parametrization of an autonomous SSM that can be continued under the addition of small external forcing (§3). Via a simplification of the resulting reduced dynamics on the non-autonomous SSM, we can directly solve for the amplitudes of the forced response, restricting our focus to oscillations near the origin. Without any further restrictions, we calculate backbone curves, stability of the forced response and the amplitude–frequency relationship explicitly (§4). We then demonstrate the performance of our explicit backbone-curve formulae in three numerical examples, on which we also compare our results to those obtained from prior methods for approximating forced responses and backbone curves (§5).

2. Set-up

We consider a general, quasi-periodically forced, nonlinear, N -degree-of-freedom mechanical system of the form

$$\text{and } \begin{cases} \mathbf{M}\ddot{\mathbf{q}} + (\mathbf{C} + \mathbf{G})\dot{\mathbf{q}} + (\mathbf{K} + \mathbf{N})\mathbf{q} + \mathbf{f}_{\text{nl}}(\mathbf{q}, \dot{\mathbf{q}}) = \varepsilon \mathbf{f}_{\text{ext}}(\Omega_1 t, \dots, \Omega_k t), & \mathbf{q} \in \mathbb{R}^N, \quad 0 \leq \varepsilon \ll 1, \\ \mathbf{f}_{\text{nl}}(\mathbf{q}, \dot{\mathbf{q}}) = \mathcal{O}(|\mathbf{q}|^2, |\mathbf{q}||\dot{\mathbf{q}}|, |\dot{\mathbf{q}}|^2), \quad \mathbf{f}_{\text{ext}}(\Omega_1 t, \dots, \Omega_k t) = \sum_{\mathbf{k} \in \mathbb{Z}^k} \mathbf{f}_{\text{ext}}^{\mathbf{k}} e^{i(\mathbf{k}, \Omega)t}, & k \geq 1, \end{cases} \quad (2.1)$$

where \mathbf{M} is a symmetric, positive-definite matrix; the stiffness matrix \mathbf{K} and the damping matrix \mathbf{C} are symmetric, positive semi-definite; the matrix of the follower forces \mathbf{N} and the gyroscopic matrix \mathbf{G} are skew-symmetric; and the nonlinear forcing vector $\mathbf{f}_{\text{nl}}(\mathbf{q}, \dot{\mathbf{q}})$ is at least quadratic in its arguments. Observe that $\mathbf{q} \equiv 0$ is an equilibrium of the unforced system ($\varepsilon = 0$). The external forcing $\varepsilon \mathbf{f}_{\text{ext}}$ does not depend on the generalized coordinates or velocities and has finitely many rationally incommensurate frequencies $(\Omega_1, \dots, \Omega_k)$. As such, \mathbf{f}_{ext} admits a convergent Fourier representation with frequency base vector $\Omega = (\Omega_1, \dots, \Omega_k)$, as indicated.

We denote the eigenvalues of the linearized system (2.1) by $\lambda_1, \dots, \lambda_{2N}$, with multiplicities and conjugates included. We assume an underdamped configuration, i.e. complex eigenvalues with non-zero imaginary part and negative real part. Owing to the importance of the eigenvalues with the smallest real part for the existence of the non-autonomous SSM (cf. [3]), we denote one of these eigenvalues by λ_{\min} and order all eigenvalues as follows:

$$\lambda_j = \bar{\lambda}_{j+N}, \quad \text{Im}(\lambda_j) > 0, \quad \text{Re}(\lambda_{\min}) \leq \text{Re}(\lambda_j) < 0, \quad j = 1, \dots, N. \quad (2.2)$$

By (2.2) the $\mathbf{q} \equiv 0$ equilibrium of the unforced limit of (2.1) is asymptotically stable. This context is relevant for vibrations of lightly damped structures.

To obtain the first-order equivalent system, we define the matrices

$$\text{and } \begin{cases} \mathbf{A} = \begin{pmatrix} 0 & \mathbf{I} \\ -\mathbf{M}^{-1}(\mathbf{K} + \mathbf{N}) & -\mathbf{M}^{-1}(\mathbf{C} + \mathbf{G}) \end{pmatrix}, \quad \mathbf{G}_{\text{nl}}(\mathbf{x}) = \begin{pmatrix} 0 \\ \mathbf{M}^{-1} \mathbf{f}_{\text{nl}}(\mathbf{x}) \end{pmatrix} \\ \mathbf{g}_{\text{ext}}^{\mathbf{k}} = \begin{pmatrix} 0 \\ \mathbf{M}^{-1} \mathbf{f}_{\text{ext}}^{\mathbf{k}} \end{pmatrix}, \quad \mathbf{G}_{\text{ext}}(\Omega_1 t, \dots, \Omega_k t) = \sum_{\mathbf{k} \in \mathbb{Z}^k} \mathbf{g}_{\text{ext}}^{\mathbf{k}} e^{i(\mathbf{k}, \Omega)t}. \end{cases} \quad (2.3)$$

By letting $\mathbf{x} = (\mathbf{q}, \dot{\mathbf{q}})$ in (2.1) and the definitions (2.3), we obtain the first-order equivalent system

$$\dot{\mathbf{x}} = \mathbf{A}\mathbf{x} + \mathbf{G}_{\text{nl}}(\mathbf{x}) + \varepsilon \mathbf{G}_{\text{ext}}(\Omega_1 t, \dots, \Omega_k t). \quad (2.4)$$

We define the matrices

$$\mathbf{A} = \text{diag}(\lambda_1, \dots, \lambda_{2N}), \quad \mathbf{V} = [\mathbf{v}_1, \dots, \mathbf{v}_{2N}], \quad \mathbf{v}_j = \begin{pmatrix} \mathbf{e}_j \\ \lambda_j \mathbf{e}_j \end{pmatrix}, \quad (2.5)$$

where \mathbf{v}_j is the eigenvector of (2.4), corresponding to the eigenvalue λ_j and to the mode shape \mathbf{e}_j of the linear part of (2.1). We assume that the matrix \mathbf{A} is semisimple and therefore $\mathbf{\Lambda} = \mathbf{V}^{-1}\mathbf{A}\mathbf{V}$ holds. An equivalent autonomous version of the non-autonomous system (2.4) can be obtained by introducing the phases

$$\phi_j = \Omega_j t, \quad j = 1, \dots, k, \quad (2.6)$$

which yield

$$\begin{pmatrix} \dot{\mathbf{x}} \\ \dot{\boldsymbol{\phi}} \end{pmatrix} = \begin{bmatrix} \mathbf{A}\mathbf{x} + \mathbf{G}_{\text{nl}}(\mathbf{x}) + \varepsilon \mathbf{G}_{\text{ext}}(\boldsymbol{\phi}) \\ \boldsymbol{\Omega} \end{bmatrix}. \quad (2.7)$$

For system (2.4) or its equivalent autonomous form (2.7), we now restate the main results of Haller & Ponsioen [3]. We consider eigenspaces of system (2.4) of the form

$$E = \text{span}\{\mathbf{v}_1, \dots, \mathbf{v}_s, \mathbf{v}_{N+1}, \dots, \mathbf{v}_{N+s}\}, \quad (2.8)$$

with their smoothest nonlinear continuation defined as follows.

Definition 2.1. A SSM, $W(E)$, corresponding to the eigenspace E defined in (2.8) is an invariant manifold of the system (2.4) with the following properties:

- (i) $W(E)$ has the same dimensions as E (i.e. $\dim(W(E)) = 2s$) and perturbs smoothly from E at $\mathbf{x} = 0$ under the addition of the nonlinear and $\mathcal{O}(\varepsilon)$ terms of system (2.4);
- (ii) $W(E)$ is strictly smoother than any other invariant manifold satisfying (i).

From now on, we assume that the non-resonance conditions

$$\sum_{j=1}^s m_j \text{Re}(\lambda_j) \neq \text{Re}(\lambda_n), \quad n = s + 1, \dots, N, \quad 2 \leq \sum_{j=1}^s m_j \leq \Sigma(E), \quad m_j \in \mathbb{N}, \quad (2.9)$$

hold, with the absolute spectral quotient $\Sigma(E)$ defined as

$$\Sigma(E) = \text{Int} \left(\frac{\text{Re}(\lambda_{\min})}{\max_{j=1, \dots, s} (\text{Re}(\lambda_j))} \right), \quad (2.10)$$

where the operator $\text{Int}(\cdot)$ extracts the integer part of its argument. Then we have the following results on the SSMs of the general mechanical system (2.4):

Theorem 2.2. Assume that the non-resonance conditions (2.9) are satisfied for an eigenspace E defined in (2.8). Then the following statements hold:

- (i) The SSM, $W(E)$, for system (2.4) uniquely exists in the class of $C^{\Sigma(E)+1}$ manifolds.
- (ii) A parametrization $\mathbf{W}: \mathbb{R}^{2s} \rightarrow \mathbb{R}^{2N}$ of the invariant manifold $W(E)$ can be approximated in a neighbourhood of the origin as a polynomial in the parametrization variable \mathbf{z} , with coefficients depending on the phase variables $\boldsymbol{\phi}$, i.e.

$$\mathbf{x} = \mathbf{W}(\mathbf{z}, \boldsymbol{\phi}), \quad \mathbf{z} \in \mathbb{R}^{2s}, \quad (2.11)$$

- (iii) There exist a polynomial function $\mathbf{R}(\mathbf{z}, \boldsymbol{\phi})$, defined on an open neighbourhood of $\mathbf{x} = 0$, such that the invariance condition

$$\mathbf{A}\mathbf{W}(\mathbf{z}, \boldsymbol{\phi}) + \mathbf{G}(\mathbf{W}(\mathbf{z}, \boldsymbol{\phi})) + \varepsilon \mathbf{G}_{\text{ext}}(\boldsymbol{\phi}) = D_{\mathbf{z}}\mathbf{W}(\mathbf{z}, \boldsymbol{\phi})\mathbf{R}(\mathbf{z}, \boldsymbol{\phi}) + D_{\boldsymbol{\phi}}\mathbf{W}(\mathbf{z}, \boldsymbol{\phi})\boldsymbol{\Omega}. \quad (2.12)$$

holds. Therefore, the dynamics on the SSM (i.e. the reduced dynamics) are governed by

$$\dot{\mathbf{z}} = \mathbf{R}(\mathbf{z}, \boldsymbol{\phi}). \quad (2.13)$$

- (iv) The parametrization $\mathbf{W}(\mathbf{z}, \boldsymbol{\phi})$, as well as the reduced dynamics $\mathbf{R}(\mathbf{z}, \boldsymbol{\phi})$, are robust with respect to changes in the parameters.

Proof. This is a restatement of the main theorem by Haller & Ponsioen [3] (Theorem 4), deduced from more abstract results on invariant manifolds of Haro & de la Lave [8] (Theorem 4.1) in our current setting. ■

If the non-resonance conditions are satisfied for the general mechanical system (2.1), theorem 2.2 establishes the existence, smoothness and uniqueness of the SSM tangent to a modal subspace of interest. Owing to the smooth persistence of the SSM with respect to the small parameter ε , the parametrization of the SSM, as well the reduced dynamics, can be expanded in ε . As the forcing in equation (2.4) is of the first order in ε , the leading-order approximations to the SSM (\mathbf{W}_0) and to the dynamics (\mathbf{R}_0) do not depend on the phase variables ϕ . Specifically, we have

$$\left. \begin{aligned} \mathbf{W}(\mathbf{z}, \phi) &= \mathbf{W}_0(\mathbf{z}) + \sum_{l=1}^{\infty} \varepsilon^l \mathbf{W}_l(\mathbf{z}, \phi) \\ \mathbf{R}(\mathbf{z}, \phi) &= \mathbf{R}_0(\mathbf{z}) + \sum_{l=1}^{\infty} \varepsilon^l \mathbf{R}_l(\mathbf{z}, \phi), \end{aligned} \right\} \quad (2.14)$$

and

where the subscripts of \mathbf{W} and \mathbf{R} indicate the order in the ε expansion. As a consequence, we have the following corollary.

Corollary 2.3. *If, in addition to the inner non-resonance conditions (2.9), the outer non-resonance conditions*

$$\sum_{j=1}^s m_j \lambda_j \neq \lambda_n, \quad n = 1, \dots, s, \quad 2 \leq \sum_{j=1}^s m_j \leq \Sigma(E), \quad m_j \in \mathbb{N}, \quad (2.15)$$

hold for the eigenspace E defined in (2.8), then $\mathbf{R}_0(\mathbf{z}, \phi)$ can be chosen linear in \mathbf{z} .

Proof. This corollary follows directly from the work of Cabré *et al.* [24] for discrete mappings (Theorem 1.1) and is also stated by Szalai *et al.* [6]. These results are applicable here because \mathbf{W}_0 and \mathbf{R}_0 are autonomous. ■

To conveniently express the polynomial expansions of $\mathbf{W}(\mathbf{z}, \phi)$ and $\mathbf{R}(\mathbf{z}, \phi)$, we use the multi-index notation

$$\left. \begin{aligned} \mathbf{W}_l(\mathbf{z}, \phi) &= \sum_{\mathbf{m} \in \mathbb{N}_0^{2s}} \mathbf{w}_l^{\mathbf{m}}(\phi) \mathbf{z}^{\mathbf{m}}, \quad \mathbf{w}_l^{\mathbf{m}} \in \mathbb{C}^{2N} \\ \mathbf{R}_l(\mathbf{z}, \phi) &= \sum_{\mathbf{m} \in \mathbb{N}_0^{2s}} \mathbf{r}_l^{\mathbf{m}}(\phi) \mathbf{z}^{\mathbf{m}}, \quad \mathbf{r}_l^{\mathbf{m}} \in \mathbb{C}^{2s}, \end{aligned} \right\} \quad (2.16)$$

where the superscript \mathbf{m} indicates the associated monomial of the coefficient vectors $\mathbf{w}_l^{\mathbf{m}}$ and $\mathbf{r}_l^{\mathbf{m}}$.

3. Spectral submanifolds for the forced system

Given a parametrization of the SSM, $W(E)$, and its reduced dynamics for the autonomous limit of (2.1) ($\varepsilon = 0$), we now consider the continuation of these under the addition of small forcing terms. We truncate the parametrization $\mathbf{W}(\mathbf{z}, \phi)$ and the associated reduced dynamics $\mathbf{R}(\mathbf{z}, \phi)$ at $\mathcal{O}(\varepsilon|\mathbf{z}|, \varepsilon^2)$. With the notation (2.16), the series expansion (2.14) of $\mathbf{W}(\mathbf{z}, \phi)$ and $\mathbf{R}(\mathbf{z}, \phi)$ can be rewritten as

$$\left. \begin{aligned} \mathbf{W}(\mathbf{z}, \phi) &= \mathbf{W}_0(\mathbf{z}) + \varepsilon \mathbf{w}_1^0(\phi) + \mathcal{O}(\varepsilon|\mathbf{z}|, \varepsilon^2) \\ \mathbf{R}(\mathbf{z}, \phi) &= \mathbf{R}_0(\mathbf{z}) + \varepsilon \mathbf{r}_1^0(\phi) + \mathcal{O}(\varepsilon|\mathbf{z}|, \varepsilon^2). \end{aligned} \right\} \quad (3.1)$$

The equations (3.1) reveal that only the unknown coefficient vectors $\mathbf{w}_1^0(\phi)$ and $\mathbf{r}_1^0(\phi)$ need to be computed to achieve the desired $\mathcal{O}(\varepsilon|\mathbf{z}|, \varepsilon^2)$ accuracy.

First, we discuss a general leading-order parametrization \mathbf{W}_0 and its dynamics \mathbf{R}_0 , then we modify this parametrization to accommodate the near-resonant nature of conjugate eigenvalue pairs that arises under weak damping (cf. [6]).

(a) General parametrization

For a general parametrization truncated at $\mathcal{O}(\varepsilon|\mathbf{z}|, \varepsilon^2)$, we state the result in the following lemma;

Lemma 3.1. *If the non-resonance conditions (2.9) are satisfied for the spectral subspace (2.8) of system (2.4), then the coefficient vectors $\mathbf{w}_1^0(\boldsymbol{\phi})$ and $\mathbf{r}_1^0(\boldsymbol{\phi})$ of parametrization $\mathbf{W}(\mathbf{z}, \boldsymbol{\phi})$ and the dynamics $\mathbf{R}(\mathbf{z}, \boldsymbol{\phi})$ are given by*

$$\mathbf{w}_1^0 = \sum_{\mathbf{k} \in \mathbb{Z}^k} \mathbf{V}(i\langle \mathbf{k}, \boldsymbol{\Omega} \rangle \mathbf{I} - \boldsymbol{\Lambda})^{-1} \mathbf{V}^{-1} \mathbf{g}_{\text{ext}}^{\mathbf{k}} e^{i\langle \mathbf{k}, \boldsymbol{\phi} \rangle} \quad (3.2a)$$

and

$$\mathbf{r}_1^0 = \mathbf{0}. \quad (3.2b)$$

Proof. The non-resonance conditions (2.9) ensure the existence of the SSM, therefore the parametrization and the reduced dynamics can be expressed in the form (2.14). Substituting this series expansion into the invariance condition (2.12) and comparing terms of equal order in ε and \mathbf{z} , we obtain the expressions (3.2a) and (3.2b). We detail this coefficient comparison in appendix Aa. ■

The specific form of \mathbf{W}_0 and \mathbf{R}_0 depends on the choice of the modal subspace (2.8). Cabré *et al.* [24] point out that the parametrization of SSM is not unique, even though the SSM is. Because of the conditions (2.2), the inverse in formula (3.2a) is non-singular. Still, if the norm of the damping matrix \mathbf{C} is small and a harmonic $\langle \mathbf{k}, \boldsymbol{\Omega} \rangle$ is near-resonant, i.e.

$$\langle \mathbf{k}, \boldsymbol{\Omega} \rangle \approx \text{Im}(\lambda_j), \quad (3.3)$$

then small denominators arise in equation (3.2a). These denominators would restrict the domain of validity of our calculations. To avoid this issue, we will eliminate small denominators by keeping terms in $\mathbf{R}(\mathbf{z}, \boldsymbol{\phi})$ that could otherwise be eliminated from the reduced dynamics.

(b) Forced response of the nonlinear mechanical system

Having identified terms that potentially contain small denominators, we continue by keeping additional terms in the reduced dynamics to ascertain that no small denominators arise in the parametrization. To construct frequency–amplitude response curves, we now assume canonical single-harmonic forcing ($k = 1$) in the form of

$$\mathbf{f}_{\text{ext}} = \mathbf{f} \cos(\Omega t) = \mathbf{f} \frac{e^{i\Omega t} + e^{-i\Omega t}}{2}. \quad (3.4)$$

Therefore, only the forcing terms $\mathbf{g}_{\text{ext}}^{\pm 1}$ (cf. equation (2.3)) are non-zero. The period of the forcing (3.4) is $T = 2\pi/\Omega$. We restrict our calculations to the case when $W(E)$ is two-dimensional ($s = 1$), which are tangent to an eigenspace

$$E_l = \text{span}\{\mathbf{v}_l, \mathbf{v}_{l+N}\}. \quad (3.5)$$

We denote the parametrization variable for the corresponding SSM $W(E_l)$ by $\mathbf{z} = [z_l, \bar{z}_l]^T$. As the eigenvalues λ_l and λ_{l+N} are complex conjugates (cf. condition (2.2)), the internal resonance conditions (2.15) are technically satisfied and the dynamics $\mathbf{R}_0(\mathbf{z})$ could be chosen linear. As noted by Szalai *et al.* [6], however, the near-resonance relationships

$$(m+1)\lambda_l + m\lambda_{l+N} \approx \lambda_l, \quad m\lambda_l + (m+1)\lambda_{l+N} \approx \lambda_{l+N}, \quad m \leq M, \quad (3.6)$$

between complex conjugate eigenvalues always hold for small damping (i.e. $2M|\text{Re}(\lambda_j)| \ll 1$). The weaker the damping, the higher the value of the positive integer M needs to be set. Removing the

corresponding terms from the dynamics would lead to small denominators in the parametrization \mathbf{W}_0 of the SSM. To this end, we keep such near-resonant terms in $\mathbf{R}_0(\mathbf{z})$ by letting

$$\mathbf{R}_0(\mathbf{z}) = \begin{bmatrix} \lambda_l z_l \\ \lambda_l \bar{z}_l \end{bmatrix} + \sum_{m=1}^M \begin{bmatrix} \beta_m z_l^{m+1} \bar{z}_l^m \\ \bar{\beta}_m z_l^m \bar{z}_l^{m+1} \end{bmatrix} + \mathcal{O}(\mathbf{z}^{2M+3}). \quad (3.7)$$

The order of the autonomous SSM and its associated dynamics in the parametrization variable \mathbf{z} is $2M + 1$. For instance, for the choice of $M = 1$, a parametrization the autonomous SSM $\mathbf{W}_0(\mathbf{z})$ and its associated dynamics $\mathbf{R}_0(\mathbf{z})$ are of order three in \mathbf{z} . For this case, a formula for the constant β_1 in (3.7) for the general mechanical system (2.4) with diagonalized linear part is given by Szalai *et al.* [6], which we recall in appendix B for completeness.

For increasing accuracy or large-amplitude oscillations it is desirable to compute (3.7) for a higher choice of M ($M > 1$). To compute the arising constants β_m of the reduced dynamics (3.7) the invariance condition (cf. appendix Aa equation (A 3)) has to be solved for a polynomial $\mathbf{W}_0(\mathbf{z})$ and $\mathbf{R}_0(\mathbf{z})$ manually or the automated computation package of Ponsioen *et al.* [7] can be used. For the calculation of the $\mathcal{O}(5)$ SSM ($M = 2$), we provide a Matlab script as the electronic supplementary material.

As for the computation of \mathbf{W}_0 in the $M = 1$ case, Szalai *et al.* [6], showed that a two-dimensional SSM, $W(E_l)$, of the unforced limit of system (2.1) can be constructed if the further non-resonance conditions

$$m_1 \lambda_l + m_2 \bar{\lambda}_l \not\approx \lambda_j, \quad j \neq l, l + N \quad \text{and} \quad 1 \leq m_1 + m_2 \leq \Sigma(E_l) \quad (3.8)$$

are satisfied.

To study the continuation of the autonomous SSM from Szalai *et al.* [6] under the addition of the small forcing terms defined in (3.4), we rescale the parametrization variable

$$\mathbf{z} \mapsto \varepsilon^{1/(2M+2)} \mathbf{z} = \mu \mathbf{z} \quad (3.9)$$

and truncate all formulae for the SSM and its reduced dynamics at order μ^{2M+3} in the following. Higher-order approximations could be obtained in a similar fashion.

To explicitly construct an approximation to the SSM, we define the matrices \mathbf{S}^+ and \mathbf{S}^- elementwise as

$$\mathbf{S}_{jm}^+ = \delta_{jm} - \delta_{lj} \delta_{lm'}, \quad \mathbf{S}^- = \delta_{jm} - \delta_{(l+N)j} \delta_{(l+N)m'}, \quad j, m = 1, \dots, 2N. \quad (3.10)$$

Both matrices (\mathbf{S}^+ and \mathbf{S}^-) equal the identity, except that the element S_{ll}^+ is zero and the $(l + N)$ th entry on the main diagonal of \mathbf{S}^- is zero. Furthermore, we denote the j th row of the inverse of the eigenvector matrix \mathbf{V} by \mathbf{t}_j , i.e.

$$[\mathbf{t}_1, \mathbf{t}_2, \dots, \mathbf{t}_{2N}] = \mathbf{V}^{-1}, \quad \mathbf{t}_j \in \mathbb{C}^{1 \times 2N}, \quad j = 1, \dots, 2N. \quad (3.11)$$

We then have the following result for the autonomous SSM and its associated reduced dynamics.

Theorem 3.2. *If the non-resonance conditions (2.9) and (3.8) hold for the subspace E_L (cf. equation (3.5)) for the general mechanical system (2.1) under the canonical single-harmonic forcing (3.4), then the $\mathcal{O}(\mu^{2M+3})$ approximation of the parametrization and its reduced dynamics can be written in the form*

$$\mathbf{W}(\mathbf{z}, \Omega t) = \mathbf{W}_0(\mathbf{z}) + \mu^{2M+2} \mathbf{w}_1^0(\Omega t) + \mathcal{O}(\mu^{2M+3}) \quad (3.12a)$$

and

$$\mathbf{R}(\mathbf{z}, \Omega t) = \mathbf{R}_0(\mathbf{z}) + \mu^{2M+2} \mathbf{r}_1^0(\Omega t) + \mathcal{O}(\mu^{2M+3}), \quad (3.12b)$$

where the coefficient vectors \mathbf{w}_1^0 and \mathbf{r}_1^0 are given by

$$\mathbf{w}_1^0 = \mathbf{V} \mathbf{S}^+ (i\Omega \mathbf{I} - \mathbf{A})^{-1} \mathbf{V}^{-1} \mathbf{g}_{\text{ext}}^{(1)} e^{i\Omega t} + \mathbf{V} \mathbf{S}^- (-i\Omega \mathbf{I} - \mathbf{A})^{-1} \mathbf{V}^{-1} \mathbf{g}_{\text{ext}}^{(-1)} e^{-i\Omega t} \quad (3.13a)$$

and

$$\mathbf{r}_1^0 = r_c \begin{bmatrix} e^{i\Omega t} \\ -e^{-i\Omega t} \end{bmatrix}, \quad r_c = \mathbf{t}_l \mathbf{g}_{\text{ext}}^{(1)}. \quad (3.13b)$$

Proof. As the non-resonance conditions (2.9) hold, the existence of the SSM can be guaranteed. Given that the additional non-resonance conditions (3.8) also hold, the result from Szalai *et al.* [6] also applies and we can select the parametrization variable such that the reduced dynamics of the autonomous limit of system (2.1) is of the form (3.7). Substituting the series expansion (2.14) and the scaling (3.9) into the invariance condition (2.12) and comparing terms of equal order in μ , we obtain equations (3.12a) and (3.12b). We solve the arising equation at order μ^{2M+2} eliminating small denominators and obtain the explicit equations for \mathbf{w}_1^0 and \mathbf{r}_1^0 (cf. equations (3.13a) and (3.13b)). We give the detailed derivations in appendix Ab. ■

Remark 3.3. The constant r_c in equation (3.13b) is the component of the forcing vector \mathbf{f} in equation (3.4) falling in the subspace E_l defined in (3.5).

Remark 3.4. As we assume non-zero real part for the eigenvalues λ_j (cf. condition (2.2)), the inverse in (3.13a) is non-singular. By construction, the matrices \mathbf{S}^\pm cancel out the terms with small denominators in the parametrization.

Remark 3.5. The non-resonance conditions (3.8) are violated for internally resonant structures. In this case, the system dynamics cannot be reduced to a two-dimensional SSM; rather, a higher-dimensional SSM needs to be constructed. Specific formulae for the reduction of an autonomous system to a higher-dimensional SSM (\mathbf{W}_0 and \mathbf{R}_0 , for $s > 1$) have not yet been obtained in the literature, even though they can, in principle, be deduced from the invariance condition (2.12).

Theorem 3.2 leads to the following corollary.

Corollary 3.6. *The eigenvectors \mathbf{v}_j can be normalized such that r_c is purely imaginary.*

Proof. The proof relies on the fact that we can multiply the eigenvectors with a complex constant such that equation (3.15) holds. We detail this in appendix Ad. ■

Remark 3.7. In the case of purely symmetric system matrices in (2.1) ($\mathbf{N} = \mathbf{0}$ and $\mathbf{G} = \mathbf{0}$) and structural damping ($\mathbf{C} = \alpha_m \mathbf{M} + \alpha_k \mathbf{K}$, $\alpha_k, \alpha_m \in \mathbb{R}$), the mode shapes \mathbf{e}_j (cf. equation (2.5)) can be mass-normalized, i.e. for the matrix of mode shapes $\mathbf{E} = [\mathbf{e}_1, \dots, \mathbf{e}_N]$

$$\mathbf{E}^{-1} \mathbf{M} \mathbf{E} = \mathbf{I} \quad (3.14)$$

holds. Then the constant r_c turns out to be always purely imaginary, which we also derive in appendix Ad.

Based on corollary 3.6, we can assume a purely imaginary constant r_c without loss of generality. We denote the imaginary part of r_c by r , i.e.

$$r = \text{Im}(r_c). \quad (3.15)$$

To determine the steady-state response of (2.1), we seek for T -periodic orbits of the reduced dynamics (3.12b). To this end, we transform the parametrization variables to polar coordinates by letting

$$z_l = \rho e^{i\theta}. \quad (3.16)$$

Furthermore, we separate the real and imaginary parts of the reduced dynamics (3.7) as

$$\text{Re}(\mathbf{R}_0(\mathbf{z})) = a(\rho) = \text{Re}(\lambda_l)\rho + \sum_{m=1}^M \text{Re}(\beta_m)\rho^{2m+1} \quad (3.17a)$$

and

$$\frac{1}{\rho} \text{Im}(\mathbf{R}_0(\mathbf{z})) = b(\rho) = \text{Im}(\lambda_l) + \sum_{m=1}^M \text{Im}(\beta_m)\rho^{2m}. \quad (3.17b)$$

By formula (3.13b), if the forcing vector \mathbf{f} is perpendicular to the subspace E_l , then r_c is zero. In that case, system (3.12b) has a fixed point at the origin, which is asymptotically stable, because of the conditions (2.2). In general, however, r is non-zero, in which case we obtain the following:

Theorem 3.8. *With the transformation (3.16) and the notation introduced in (3.17a) and (3.17b), the following specific expressions for T -periodic orbits of the reduced dynamics (3.12b) on the time-dependent SSM $W(E_1)$ for non-zero r hold:*

- (i) *Amplitude of the periodic response: The amplitudes of the T -periodic orbits of (3.12b) are given by the zeros of the equation*

$$f(\rho, \Omega) := [a(\rho)]^2 + [b(\rho) - \Omega]^2 \rho^2 - \varepsilon^2 r^2. \quad (3.18)$$

- (ii) *Phase shift of the periodic response: For a given amplitude ρ of the periodic response, the phase shift ψ between the T -periodic orbit and the external forcing \mathbf{f}_{ext} is*

$$\psi = \arccos\left(\frac{[\Omega - b(\rho)]\rho}{\varepsilon r}\right). \quad (3.19)$$

- (iii) *Stability of the periodic response: The stability of the T -periodic response with amplitude ρ is determined by the eigenvalues of the Jacobian*

$$\mathbf{J}(\rho) = \begin{bmatrix} \frac{\partial a(\rho)}{\partial \rho} & [\Omega - b(\rho)]\rho \\ \frac{\partial b(\rho)}{\partial \rho} - \frac{\Omega - b(\rho)}{\rho} & \frac{a(\rho)}{\rho} \end{bmatrix}. \quad (3.20)$$

Proof. This result can be deduced by substitution of the transformation (3.16) into the reduced dynamics (3.12b) and solving the resulting equations for T -periodic orbits. We carry out these computations in detail in appendix Ad. ■

The constants β_m , necessary to compute $a(\rho)$ and $b(\rho)$, can be obtained from the invariance of the SSM (cf. equation (2.12)). Depending on the order of the SSM (M) specific formulae for β_m can be taken from Szalai *et al.* [6] or appendix B ($M=1$), the Matlab script provided as the electronic supplementary material ($M=2$) or the automated computation package of Ponsioen *et al.* [7].

4. Analytic results on backbone curve, periodic responses and their stability

Having derived condensed formulae for the amplitude (3.18) and the stability (3.20) of the forced response of system (2.1), we can now analytically compute backbone curves and stability regions. Furthermore, we obtain below the forced response in physical coordinates.

(a) Backbone curve

As mentioned in the Introduction various definitions of the backbone curve can be found in the literature. The definition by Klotter [19], as the frequency–amplitude relationship of the conservative unforced limit, was adopted by Rosenberg & Atkinson [20]. This definition, however, has two major drawbacks. First, a general justification for the relevance of this curve for the response of the forced-damped system (2.1) is not available to the best of our knowledge. Furthermore, due to the no-damping assumption, it is challenging to observe this curve experimentally. The definition by Nayfeh & Mook [16] and Cveticanin *et al.* [17] of the backbone curve as the curve connecting points of maximal response amplitude as a function of an external forcing frequency, defines a relevant and experimentally observable curve. We formalize this definition here as follows.

Definition 4.1. The *backbone curve* of the mechanical system (2.1) is the curve of maximal amplitude of the periodic response on the SSM (3.12a) as a function of the frequency of the external forcing (3.4).

The function (3.18) relates implicitly the response amplitude ρ with the forcing amplitude r and frequency Ω , and hence summarizes information about a whole family of response curves. The maximal amplitude location of each such curve is a single point on the backbone curve by

definition 4.1. By definition 4.1, points on the backbone curve can be identified by equating the derivative of the amplitudes with respect to the forcing frequency Ω with zero. To find these locations, first note that implicit differentiation of (3.18) gives

$$\frac{\partial f(\rho, \Omega)}{\partial \Omega} = -2(b(\rho) - \Omega)\rho^2. \quad (4.1)$$

To identify the frequency $\Omega = \Omega_{\max}$, at which the amplitude of the forced response of (2.1) is at a maximum, we equate the expression (4.1) with zero. Solving for Ω_{\max} from the resulting equation, we obtain

$$\Omega_{\max}(\rho_{\max}) = b(\rho_{\max}) = \text{Im}(\lambda_l) + \sum_{m=1}^M \text{Im}(\beta_m)\rho_{\max}^{2m}. \quad (4.2)$$

The maximal response amplitude ρ_{\max} parametrizes the backbone curve. The phase shift between response and excitation along the backbone curve is given by

$$\psi(\rho_{\max}) = \frac{\pi}{2}, \quad (4.3)$$

as one obtains from (3.19) by substituting $\rho = \rho_{\max}$ and $\Omega = \Omega_{\max}$. Peeters *et al.* [18] derived a similar 90° phase lag, under the assumption of structural damping. Equation (4.3) confirms this conclusion for any damping, that is a polynomial function of positions and velocities.

The SSM construction described by Haller & Ponsioen [3] for dissipative systems does not apply to conservative mechanical systems as the $\mathbf{q} = 0$ equilibrium is not hyperbolic in that case. The Lyapunov subcentre-manifold theorem for autonomous conservative systems (cf. [25]), however, guarantees the existence of an unique analytic invariant manifold tangent to the modal subspace (3.5) under appropriate non-resonance conditions. These Lyapunov subcentre-mainfolds (LSMs) are then filled with periodic orbits. If, in addition to the forcing, the linear and nonlinear damping are also of first order in ε , the $\varepsilon \rightarrow 0$ limit of system (2.1) is conservative and unforced. Then, by the uniqueness of the LSM (cf. [25]) and the continuity of the expansions (2.14) of the SSM, it is reasonable to expect that the SSM limits on the LSM. A mathematical proof for this expectation, however, is not available yet.

We obtain the conservative limit of the reduced dynamics (3.12b) by taking the limits $\varepsilon \rightarrow 0$, $\text{Re}(\lambda_l) \rightarrow 0$ and $\text{Re}(\beta_m) \rightarrow 0$ ($m = 1, \dots, M$). Transforming this limit to polar coordinates, we obtain the same frequency–amplitude relationship as given by the backbone curve (4.2). Therefore, we can confirm analytically that the frequency–amplitude relationship of the conservative limit is an $\mathcal{O}(\mu^{2M+3})$ approximation to actual backbone curve. The closeness of the two curves assumed by, e.g. the resonance decay method, has only been argued heuristically by Peeters *et al.* [18].

We further note that the backbone curve (4.2) is the same as derived by Szalai *et al.* [6], who define the backbone curve as the frequency–amplitude relationship of the decaying response along an SSM. From their calculations, however, the relevance of this curve to the forced response of system (2.1) is not immediate. Our derivations clarify here this relevance.

The backbone curve (4.2) is independent of the forcing amplitude. This fact is clear for the undamped and unforced frequency–amplitude relationship, as there is no forcing in the system, but the same result also follows directly from our analytical calculations for the damped-forced mechanical system (2.1). The forcing amplitude determines the location along the backbone curve, where the maximum of the response curve can be found. To obtain the maximum response amplitude for a given forcing, equation (3.18) has to be solved. Along the backbone curve (3.18) simplifies to

$$f(\rho_{\max}) = \left[\text{Re}(\lambda_l)\rho_{\max} + \sum_{m=1}^M \text{Re}(\beta_m)\rho_{\max}^{2m+1} \right]^2 - \varepsilon^2 r^2, \quad (4.4)$$

which can have multiple solutions for ρ_{\max} .

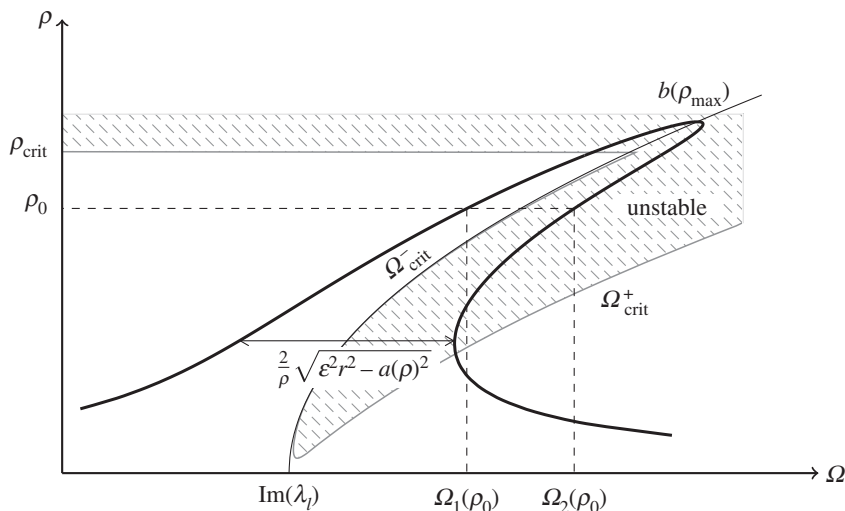


Figure 1. Sketch of a typical forced response for a third-order SSM approximation ($M = 1$) and a nonlinearity with a stiffening effect ($\text{Im}(\beta_1) > 0$).

We obtain a parametrization of the forced response in the (ρ, Ω) parameter space, by solving equation (3.18) for Ω :

$$\Omega(\rho) = b(\rho) \pm \frac{1}{\rho} \sqrt{\epsilon^2 r^2 - a(\rho)^2}, \quad (4.5)$$

where only real values of Ω are meaningful. Equation (4.5) reveals that the forced response is symmetric with respect to the backbone curve (cf. figure 1). For a given amplitude $\rho = \rho_0$ one or two forced responses with that amplitude may exist. If there is only one such response, it must lie on the backbone curve (4.2).

In practice, the forcing frequency Ω is known and the amplitude ρ needs to be determined as a function of Ω , by solving for the zeros of the function (3.18). If the order of the SSM $W(E_I)$ is three ($M = 1$), we can solve (3.18) for ρ analytically. For higher-order approximations to $W(E_I)$, such an analytic solution is unavailable and hence numerical solvers must be used.

(b) Stability of the periodic response

To obtain stability regions of the forced response, we apply the Routh–Hurwitz criterion to the Jacobian (3.20). We conclude that

$$\text{Re}(\lambda_l) + \sum_{m=1}^M (m+1) \text{Re}(\beta_m) \rho^{2m} < 0 \quad (4.6)$$

and

$$\frac{a(\rho)}{\rho} \frac{\partial a(\rho)}{\partial \rho} < [\Omega - b(\rho)] \left[\rho \frac{\partial b(\rho)}{\partial \rho} - (\Omega - b(\rho)) \right] \quad (4.7)$$

must hold to ensure the asymptotic stability of the forced response. At bifurcations of the response, the inequalities (4.6) and (4.7) become equalities. According to (4.6), up to M bifurcation values for ρ_{crit} may arise. These bifurcations appear along straight lines in the (ρ, Ω) parameter space. From equation (4.7), we obtain that these lines satisfy the equations

$$\Omega_{\text{crit}}^{\pm}(\rho) = b(\rho) + \sum_{m=1}^M m \text{Im}(\beta_m) \rho^{2m} \pm \sqrt{\left[\sum_{m=1}^M m \text{Im}(\beta_m) \rho^{2m} \right]^2 - \frac{a(\rho)}{\rho} \frac{\partial a(\rho)}{\partial \rho}}. \quad (4.8)$$

These functions divide the (ρ, Ω) parameter into stable and unstable regions, as indicated in figure 1. If the real parts of the parameters β_m are zero or small ($a(\rho) \approx 0$), the graph of Ω_{crit}^- coincides with the backbone curve (cf. figure 1).

(c) The periodic response in physical coordinates

Periodic orbits of (3.12b) are related to periodic orbits in the original physical coordinates via the parametrization (3.12a). Along the periodic response, the parametrization variable is a complex exponential with amplitude ρ and with the frequency equal to the excitation frequency Ω (cf. equation (3.16)). We insert this exponential into the leading-order expression \mathbf{W}_0 for the SSM $W(E_l)$. As \mathbf{W}_0 is a polynomial of z_l and \bar{z}_l (cf. equation (2.16)), substitution of complex exponential creates higher harmonics ($m\Omega$), whereas the amplitude ρ is exponentiated.

Through the time-varying parametrization \mathbf{w}_1^0 , terms for the first harmonic arise (cf. equation (3.13a)), with their amplitudes given by

$$\mathbf{W}^\pm = \mathbf{V} \mathbf{S}^\pm (\pm i\Omega \mathbf{I} - \mathbf{A})^{-1} \mathbf{V}^{-1} \mathbf{g}^{\pm 1}. \quad (4.9)$$

With that notation we obtain for the complex amplitudes $\mathbf{x}_{j\Omega}$ of the j th harmonic of the forcing frequency Ω as

$$\mathbf{x}_{j\Omega} = \begin{cases} \sum_{m=0}^M \rho^{2m+j} e^{j i \psi(\rho)} \mathbf{w}_0^{(m+j,m)} + \delta_{1j} \varepsilon \mathbf{W}^+, & 0 \leq j \leq M, \\ \sum_{m=0}^M \rho^{2m+j} e^{-j i \psi(\rho)} \mathbf{w}_0^{(m,m+j)} + \delta_{-1j} \varepsilon \mathbf{W}^-, & -M \leq j < 0, \end{cases} \quad (4.10)$$

where the coefficients $\mathbf{w}_0^{(m+j,m)}$ are set to zero if the corresponding coefficient is higher than the computed order of \mathbf{W}_0 ($2m+j > 2M+1$). From these formulae, one obtains the amplitudes and phases of the response for the fundamental ($|j|=1$) and superharmonic ($|j|>1$) frequencies. The case $j=0$ implies a static shift of the centre of the steady-state solution, which is a known phenomenon for nonlinear system (2.1) with quadratic stiffness terms (cf. [16]).

5. Numerical examples

We now demonstrate our SSM-based analytic results on forced responses and backbone curves on three numerical examples. The first is a 2 degrees of freedom (DOF) oscillator introduced by Shaw & Pierre [2], modified and further studied by Haller & Ponsioen [3] and Szalai *et al.* [6]. The nonlinearity in this oscillator arises from a single cubic spring. Our second example, taken from Touzé & Amabili [15], also has 2 DOF, but its nonlinearities are more complex, consisting of both quadratic and cubic terms. To demonstrate the applications of our results to higher-dimensional systems, we select a chain of oscillators with 5 DOF for the third example.

On these three examples, we compare our results with the second-order normal form approach of Neild & Wagg [14] and with a normal form-type method of Touzé & Amabili [15]. Both methods assume that the mechanical system is expressed in modal coordinates and hence the linear part of the system is fully decoupled.

The Neild-Wagg method introduces a time-dependent transformation to remove forcing terms from all modal coordinates whose eigenfrequencies are not in resonance with the forcing frequency. Afterwards, it identifies the resonant terms in the dynamics via harmonic balance. Two major differences to the present approach are the treatment of damping and the nonlinearities. Specifically, Neild & Wagg [14] assume small nonlinearities and allow only small viscous damping. Neild *et al.* [4] also add an trivial dynamical equation for the time evaluation of the damping coefficients. Afterwards they carry out the normal form transformations for the enlarged system and obtain that the linear modal damping can be added to the final dynamical equations. Therefore, no transfer of linear damping between the modal coordinates induced

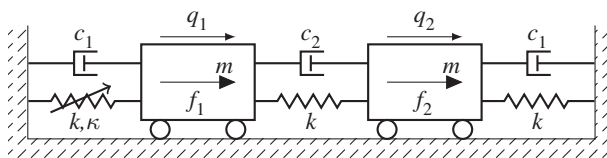


Figure 2. The modified Shaw-Pierre example discussed in [6]. We select the non-dimensional parameters $m = 1$, $k = 1$, $c_1 = \sqrt{3}c_2 = 0.003$ and $\kappa = 0.5$.

by the nonlinearities can be captured. Next, the method employs the harmonic balance to approximate the amplitude of the forced response, which leads to an expression similar to equation (3.18). Stability conditions for the steady-state solution can be found in Wagg & Neild [26] and a recent overview in Neild *et al.* [4].

By contrast, the Touzé-Amabili method starts with the unforced and damped mechanical systems in modal coordinates with geometric (position-dependent) nonlinearities. After a cubic transformation to normal form-type dynamical equations, they restrict their calculations to a subset of coordinates, called the master coordinates. The choice of the master coordinates is motivated heuristically. External forcing is then introduced directly into the normal form, representing simple forcing along non-physical, curvilinear coordinates. In addition, the forcing is assumed to be along the master coordinates only. Therefore, one can only achieve model reduction via this method, if the non-master modal coordinates are unforced, as we highlight in example 3. We acknowledge the possibility to modify the Touzé-Amabili method to overcome this shortcoming by neglecting inconvenient forcing terms. Such a reasoning, however, is not available in the literature and it is beyond the scope of this study to modify existing methods. We, therefore, follow the method as it is stated in Touzé & Amabili [15]. In analogy with Kerschen *et al.* [27] and Touzé & Amabili [15] we will obtain the forced response of the reduced dynamics via numerical continuation.

To compare the accuracy of these two methods to ours, we use the Matcont toolbox [28] of Matlab to calculate the periodic responses in the three examples directly. The result of the continuation are T -periodic orbits in the full phase space. As routinely done in the vibrations literature (cf. [4,15,18,27]), the maximal displacement along a modal direction is taken as the modal amplitude of the first harmonic. To validate the formulae for higher harmonics (cf. (4.10) for $|j| > 1$), we extract higher harmonics via the fast Fourier transformation (FFT) of selected orbits.

(a) Modified Shaw-Pierre example

Shown in figure 2, this mechanical system was originally introduced by Shaw & Pierre [2], with modifications appearing in Haller & Ponsioen [3] and Szalai *et al.* [6]. Its equations of motion are

$$\begin{bmatrix} m & 0 \\ 0 & m \end{bmatrix} \begin{bmatrix} \ddot{q}_1 \\ \ddot{q}_2 \end{bmatrix} + \begin{bmatrix} c_1 + c_2 & -c_2 \\ -c_2 & c_1 + c_2 \end{bmatrix} \begin{bmatrix} \dot{q}_1 \\ \dot{q}_2 \end{bmatrix} + \begin{bmatrix} 2k & -k \\ -k & 2k \end{bmatrix} \begin{bmatrix} q_1 \\ q_2 \end{bmatrix} + \begin{bmatrix} \kappa q_1^3 \\ 0 \end{bmatrix} = \begin{bmatrix} f_1 \\ f_2 \end{bmatrix}. \quad (5.1)$$

The system is of the general form (2.1) and hence the approach developed here applies. The eigenvalues and mode shapes of the linearized dynamics at $q_1 = q_2 = 0$ are

$$\begin{aligned} \lambda_{1,3} &= -D_1\omega_1 \pm i\omega_1\sqrt{1 - D_1^2} & \omega_1 &= \sqrt{\frac{k}{m}}, & D_1 &= \frac{c_1}{2\sqrt{km}}, & \mathbf{e}_1 &= \frac{1}{\sqrt{2}} \begin{bmatrix} 1 & 1 \end{bmatrix}^T, \\ \lambda_{2,4} &= -D_2\omega_2 \pm i\omega_2\sqrt{1 - D_2^2} & \omega_2 &= \sqrt{\frac{3k}{m}}, & 2D_2 &= \frac{c_1 + 2c_2}{\sqrt{12km}}, & \mathbf{e}_2 &= \frac{1}{\sqrt{2}} \begin{bmatrix} 1 & -1 \end{bmatrix}^T. \end{aligned}$$

For sufficiently small damping the strengthened non-resonance conditions (3.8) hold. By choosing $c_1 = \sqrt{3}c_2$, the conditions (2.9) are satisfied and hence two non-autonomous SSMs exist. The

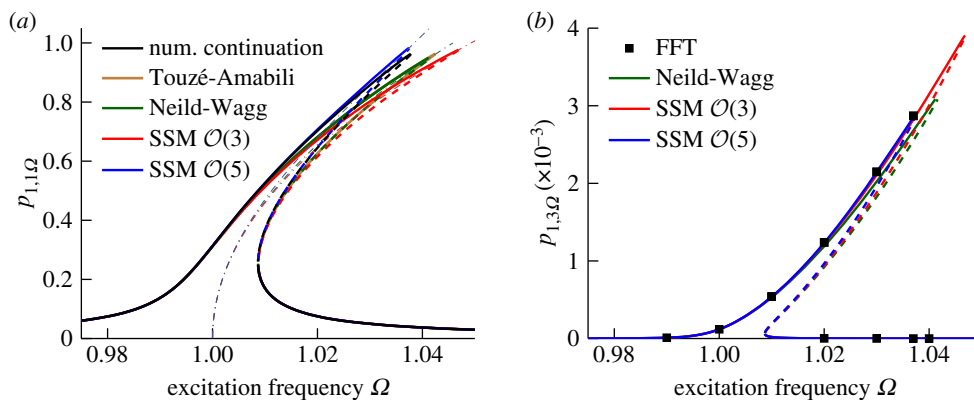


Figure 3. Response curves (thick lines) and backbone curves (thin dash-dotted lines) for example 1 under forcing of the first mode; solid lines imply stability and dashed lines instability of the forced response; parameters: $m = 1$, $k = 1$, $c_1 = \sqrt{3}c_2 = 0.003$, $\kappa = 0.5$, $f_1 = f_2 = \varepsilon/\sqrt{2} \cos(\Omega t)$ and $\varepsilon = 0.003$. (a) First harmonic and (b) third harmonic.

unforced limit of these SSMs and their reduced dynamics have already been calculated by Szalai *et al.* [6].

To apply the Touz\u00e9-Amabili method, we have to assume forcing along one of the modal coordinates only. First, we investigate forcing along the first modal coordinate $f_1 = f_2 = \varepsilon/\sqrt{2} \cos(\Omega t)$ with the amplitude $\varepsilon = 0.003$. We plot the first and third harmonics of the first modal amplitude ($p_{1,1\Omega}$ and $p_{1,3\Omega}$) in figure 3. For comparison, we show the results obtained from the Neild-Wagg method, the Touz\u00e9-Amabili method and numerical continuation with the Matlab toolbox Matcont [28] in figure 3a, with the later serving as a benchmark to hit. We indicate unstable periodic orbits in dashed lines.

While all three methods give results close to the numerical continuation, the $\mathcal{O}(5)$ SSM is the most accurate. This approach, however, is of higher order than the others. The Touz\u00e9-Amabili method can, in principle, be extended to higher orders in the coordinates but it assumes modal forcing. To improve the results of the Neild-Wagg method, one would also need to include higher-order terms in their perturbation approach, which would complicate the calculations significantly. To our best knowledge, higher-order estimates have only been obtained for 1 DOF oscillators (cf. [26,29]). Out of all third-order methods, the $\mathcal{O}(3)$ SSM computation gives the weakest result.

Touz\u00e9 & Amabili [15] do not explicitly estimate the amplitudes of higher harmonics of the forced response of system (2.1), hence the omission of the results from their method in figure 3b. Note that a periodic solution to their reduced dynamics contains fundamental and higher harmonics, which could be related to amplitudes in physical coordinates via their normal-form transformation. Here, however, we follow the published results of Touz\u00e9 & Amabili [15] without modifications.

The reference solution is generated by the FFT of the continuation signal. Again, all four results agree closely, but the $\mathcal{O}(5)$ SSM method matches the reference solution the best. Owing to the cubic nonlinearity, the modal amplitudes at even harmonics are zero for the accuracy investigated in this article.

Next, we apply forcing along the second modal degree of freedom ($l = 2$), by selecting $f_1 = -f_2 = \varepsilon/\sqrt{2} \cos(\Omega t)$ and $\varepsilon = 0.01$. We show the first and third harmonics of the computed forced response in figure 4. Again, the $\mathcal{O}(5)$ SSM approach approximates the benchmark solution most accurately. The results from the other methods are nearby and align closely with each other.

(b) Spring system

Our second example involves a mass suspended via a vertical and a horizontal spring to the wall (cf. figure 5). Touz\u00e9 *et al.* [30] derive the equation of motion for this system up to third order. With

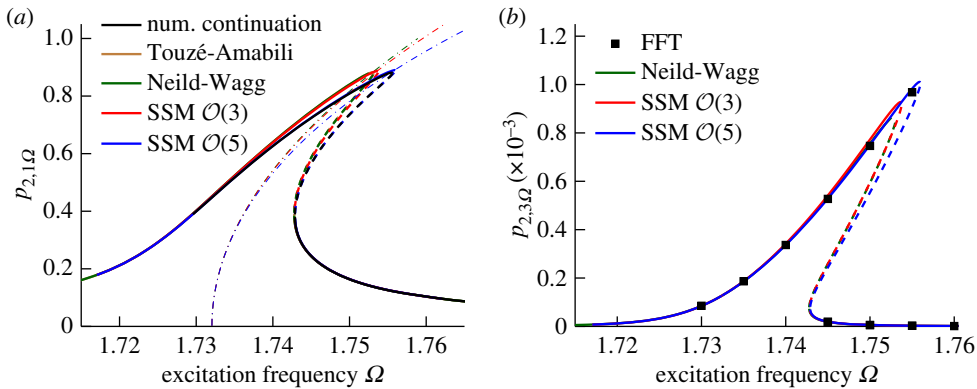


Figure 4. Response curves (thick lines) and backbone curves (thin dash-dotted lines), for example 1 under forcing of the second mode; solid lines imply stability and dashed lines instability of the forced response; parameters: $m = 1, k = 1, c_1 = \sqrt{3}c_2 = 0.003, \kappa = 0.5, f_1 = -f_2 = \varepsilon/\sqrt{2} \cos(\Omega t)$ and $\varepsilon = 0.01$. (a) First harmonic and (b) third harmonic.

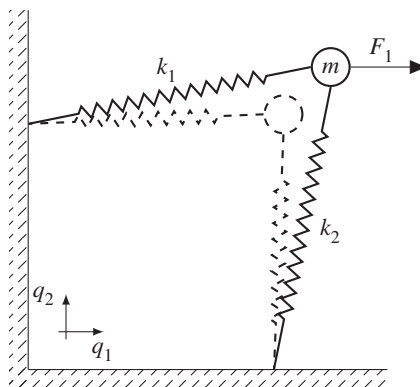


Figure 5. The mechanical system in example 2, discussed by Touzé & Amabili [15].

viscous damping and non-dimensional parameters, the equations of motion subject to horizontal forcing are

$$\left. \begin{aligned}
 \ddot{q}_1 + 2D_1\omega_1\dot{q}_1 + \omega_1^2q_1 + \frac{\omega_1^2}{2}(3q_1^2 + q_2^2) + \omega_2^2q_1q_2 + \frac{\omega_1^2 + \omega_2^2}{2}q_1(q_1^2 + q_2^2) &= F_1 = f_1 \cos(\Omega t) \\
 \text{and } \ddot{q}_2 + 2D_2\omega_2\dot{q}_2 + \omega_2^2q_2 + \frac{\omega_2^2}{2}(3q_2^2 + q_1^2) + \omega_1^2q_1q_2 + \frac{\omega_1^2 + \omega_2^2}{2}q_2(q_1^2 + q_2^2) &= 0.
 \end{aligned} \right\} \tag{5.2}$$

We choose the form of the damping and forcing for a direct comparison with Touzé & Amabili [15], but the theory developed here also applies to nonlinear damping and general forcing (see figure 5)

We select the parameters $\omega_1 = 2, \omega_2 = 4.5, D_1 = 0.01, D_2 = 0.2$ and f_1 is set to 0.02. In figure 6, we plot the amplitude of the coordinate q_1 at the first harmonic. Again, the results from numerical continuation serve as the benchmark solution. The SSMs of order three and five and the results from the Touzé-Amabili method agree well and show the same qualitative behaviour as the benchmark solution. The Neild-Wagg method incorrectly predicts hardening behaviour of the backbone curve and overestimates the amplitude. The latter arises because of the treatment of the damping by the Neild-Wagg method. In their method, modal damping is added directly

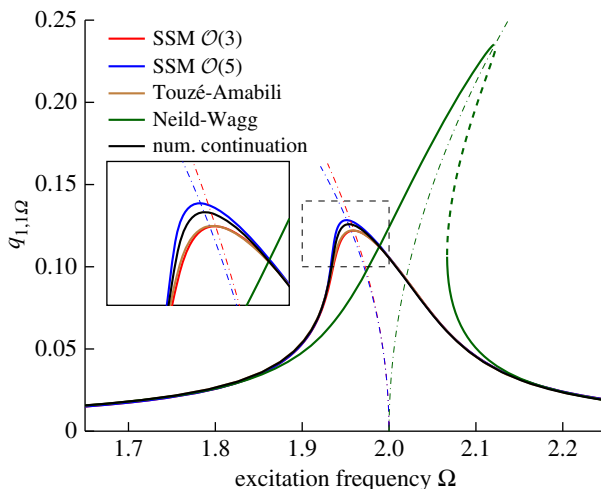


Figure 6. Amplitude of the first harmonic of the displacement q_1 (thick lines) and backbone curves (thin dash-dotted lines); solid lines imply stability and dashed lines instability of the forced response; parameters: $\omega_1 = 2$, $\omega_2 = 4.5$, $D_1 = 0.01$, $D_2 = 0.2$ and $f_1 = 0.02$.

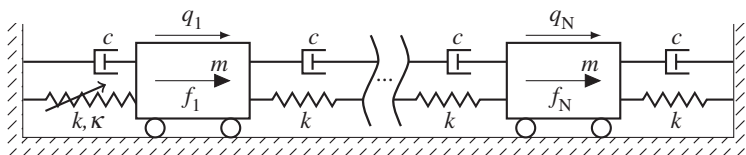


Figure 7. The oscillator chain in example 3.

to the normal form (cf. [4]) and no transfer of the linear modal damping via nonlinearities arises. Without referring to this specific method, Touz\u00e9 & Amabili [15] point out this issue for another method that incorporates damping in a similar manner. The incorrect bending behaviour arises due to the assumption of small nonlinearities, based on which all quadratic terms of nonlinearities are neglected for the backbone curve estimation in the Neild-Wagg method. To recover the effect of quadratic nonlinearities on the backbone curve, a higher-order extension in their perturbation approach is required, which would complicate the calculations significantly and is unavailable in the literature at this time. In summary, the small damping and small nonlinearity assumption made in the Neild-Wagg method is, therefore, not justified for this example.

Enlarging the frequency response curve for high amplitudes (inset in figure 6), we observe that the $\mathcal{O}(5)$ SSM construction shows the highest accuracy again. The results from the $\mathcal{O}(3)$ SSM and those from the Touz\u00e9-Amabili method almost coincide.

(c) Oscillator chain

As an application to a higher-dimensional system, we extend example 1 (cf. figure 2) into a chain of coupled oscillators. The first and the last mass are suspended to the wall, as shown in figure 7. We assume a cubic nonlinearity for the spring suspending the first mass to the wall.

The equation of motion of the j th oscillator, pictured in figure 7, is

$$m\ddot{q}_j + c(2\dot{q}_j - \dot{q}_{j+1} - \dot{q}_{j-1}) + k(2q_j - q_{j+1} - q_{j-1}) + \delta_{1j}\kappa q_j^3 = f_j(t), \quad j = 1, \dots, N. \quad (5.3)$$

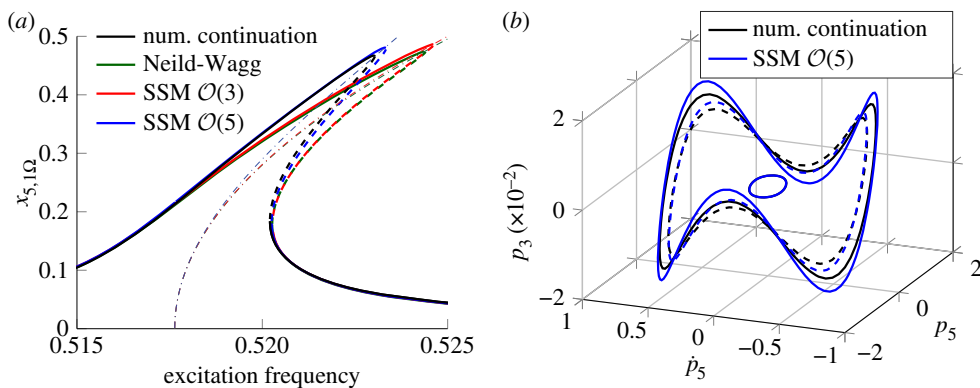


Figure 8. Results for example 3 with $N = 5$ DOF solid lines imply stability and dashed lines instability of the forced response; parameters: $m = 1$, $k = 1$, $c = 0.005$, $\kappa = 0.5$, $f_j = \delta_{1j}\varepsilon \cos(\Omega t)$ and $\varepsilon = 0.004$. (a) Amplitude of the first harmonic of the displacement of the fifth mass and backbone curves for forcing frequencies in the vicinity of the lowest eigenfrequency ($\omega_1 \approx 0.518$) and (b) periodic orbits (two stable, one unstable) for the excitation frequency $\Omega = 0.522$, projected in the modal subspace spanned by p_5 , \dot{p}_5 and p_3 .

We consider the configuration $m = 1$, $c = 0.005$, $k = 1$ and $\kappa = 0.5$, with the number of DOF set to $N = 5$. For this choice of the parameters, the natural frequencies and modal damping values are

$$\frac{j}{\omega_j^2} \left| \begin{array}{ccccc} 1 & 2 & 3 & 4 & 5 \\ 2 - \sqrt{3} & 1 & 2 & 3 & 2 + \sqrt{3} \end{array} \right., \quad D_j = \frac{c}{2}, \quad j = 1, \dots, N. \quad (5.4)$$

The non-resonance conditions (2.9) and (3.8) are satisfied for $l=1$ and hence the two-dimensional time-varying SSM exists. We assume forcing at the first mass ($f_1 = \varepsilon \cos(\Omega t)$ and $f_j = 0$ $j = 2, \dots, N$). The frequency is chosen to be close to the lowest eigenfrequency ($\omega_1 \approx 0.518$) and the amplitude is set to be $\varepsilon = 0.004$. The amplitudes of the first harmonic of the fifth coordinate $q_{5,1\Omega}$ are plotted in figure 6.

As the forcing is not aligned with a set of modal coordinates the unmodified Touzé-Amabili method is inapplicable in this example, and hence will be omitted in our comparison. Again, the $\mathcal{O}(5)$ SSM matches most accurately with the benchmark solution, obtained via numerical continuation. The frequency response curves from the SSM $\mathcal{O}(3)$ and the Neild-Wagg method deviate from the benchmark solution.

Even specific orbits computed from the analytic SSM expression match closely with the orbits obtained by numerical continuation (cf. figure 8b).

6. Conclusion

We have derived highly accurate analytic expressions for the forced response and backbone curves of damped and forced nonlinear mechanical systems of arbitrary dimension. Our procedure constructs an approximation for the two-dimensional, non-autonomous SSMs that act as nonlinear continuations of modal subspaces of the linearized system. The existence, uniqueness and smoothness of the SSMs are guaranteed under low-order non-resonance condition on the eigenvalues of the linearization (cf. [3]). We establish that a given autonomous (time-independent) SSM can be continued for the externally forced system, unless the forcing is in resonance with an imaginary part of an eigenvalue of the linearized system.

For backbone curve calculations, we focus on such resonant external forcing and construct a two-dimensional non-autonomous SSM. Constructing the SSM via the parametrization method (cf. [24]), the reduced dynamics is simplified significantly. Owing to this simplification, we are able to derive a polynomial expression whose zeros determine the amplitudes of the forced

response. Furthermore, we calculate backbone curves, stability regions and discover a symmetry of the forced response.

With our analytical treatment, we confirm the 90° phase lag criterion of the response at the backbone from Peeters *et al.* [18] for any damping that is a polynomial function of the velocities and positions. Furthermore, we connect the backbone curve, directly computed from the forced response, to the frequency–amplitude relationship of the conservative unforced limit of the system.

We demonstrate the performance of our results on three numerical examples. Comparing with the Neild-Wagg method [14], the Touzé-Amabili method [15] and numerical continuation, we conclude an overall superior performance for the $\mathcal{O}(5)$ SSM approach. While our method is applicable to general single harmonic external forcing, a model-order reduction with the Touzé-Amabili method is only achievable for forcing along a modal direction. Investigating example 2, where the nonlinearities are of quadratic and cubic form, we discover incorrect predictions from the Neild-Wagg method.

Ponsioen *et al.* [7] describe an automated computational algorithm to approximate two-dimensional SSMs of nonlinear mechanical systems up to arbitrary order. To increase the precision of our results further, these high-order approximations, can be coupled with the results of this article, which is our ongoing effort.

We have limited our discussion to two-dimensional SSMs. For multi-frequency forcing in resonance with multiple eigenvalues of the linearized system, or for structures whose eigenfrequencies are integer multiples of each other (i.e. equation (3.8) is violated), a reduction to a higher-dimensional SSM is necessary. As the theory developed by Cabré *et al.* [24] and Haro & de la Llave [8] applies to higher-dimensional submanifolds, our calculations can be extended to the multi-frequency setting.

Data accessibility. A Matlab script to compute the $\mathcal{O}(5)$ autonomous SSM ($M=2$) is available at https://github.com/tbreunung/Auto_SSM_O5.

Authors' contributions. Both authors contributed equally to this work.

Competing interests. We have no competing interests.

Funding. We received no funding for this study.

Acknowledgements. We are grateful to Florian Kogelbauer for helpful discussions and for pointing out an error in an earlier stage of this work. We are also thankful to Cyril Touzé for helpful suggestions and clarifications on his method.

Appendix A. Derivations

(a) Derivations for the spectral submanifolds of the forced system

The results stated in (3.2a) and (3.2b) follow from the work of Haller & Ponsioen [3] or Haro *et al.* [8]. Both results are generally applicable to system (2.1), because the trivial fixed point of the unforced equation (2.1) is hyperbolic (cf. conditions (2.2)). As we assume that the non-resonance conditions (2.9) hold, an SSM associated with the modal subspace E uniquely exists and persists for small $\varepsilon \geq 0$. Haro & de la Llave [8] formulate their main results for discrete mappings, but also show the direct applicability of their results to flow maps of continuous systems.

To calculate a parametrization $\mathbf{W}(\mathbf{z}, \phi)$ and the associated reduced dynamics $\mathbf{R}(\mathbf{z}, \phi)$, we start from the invariance condition (2.12) in which we substitute the series expansion (2.14). With the notation (2.16), the series expansion (2.14) can be rewritten as

$$\left. \begin{aligned} \mathbf{W}(\mathbf{z}, \phi) &= \mathbf{W}_0(\mathbf{z}) + \varepsilon \mathbf{W}_1(\mathbf{z}, \phi) + \mathcal{O}(\varepsilon^2) = \mathbf{W}_0(\mathbf{z}) + \varepsilon \mathbf{w}_1^0(\phi) + \mathcal{O}(\varepsilon|\mathbf{z}|, \varepsilon^2) \\ \text{and} \quad \mathbf{R}(\mathbf{z}, \phi) &= \mathbf{R}_0(\mathbf{z}) + \varepsilon \mathbf{R}_1(\mathbf{z}, \phi) + \mathcal{O}(\varepsilon^2) = \mathbf{R}_0(\mathbf{z}) + \varepsilon \mathbf{r}^0(\phi) + \mathcal{O}(\varepsilon|\mathbf{z}|, \varepsilon^2). \end{aligned} \right\} \quad (\text{A } 1)$$

Substituting the expansion (A 1) in the invariance condition (2.12), we obtain

$$\begin{aligned} & \mathbf{A}(\mathbf{W}_0(\mathbf{z}) + \varepsilon \mathbf{W}_1(\mathbf{z}, \phi)) + \mathbf{G}_{\text{nl}}(\mathbf{W}_0(\mathbf{z}) + \varepsilon \mathbf{W}_1(\mathbf{z}, \phi)) + \varepsilon \mathbf{G}_{\text{ext}}(\phi) \\ &= \frac{\partial \mathbf{W}_0(\mathbf{z})}{\partial \mathbf{z}} \mathbf{R}_0(\mathbf{z}) + \varepsilon \left(\frac{\partial \mathbf{W}_1(\mathbf{z}, \phi)}{\partial \mathbf{z}} \mathbf{R}_0(\mathbf{z}) + \frac{\partial \mathbf{W}_0(\mathbf{z})}{\partial \mathbf{z}} \mathbf{R}_1(\mathbf{z}, \phi) + \frac{\partial \mathbf{W}_1(\mathbf{z})}{\partial \phi} \Omega \right) + \mathcal{O}(\varepsilon^2). \end{aligned} \quad (\text{A } 2)$$

Comparing equal orders of ε , we find that the zeroth-order part of (A 2) does not contain forcing terms:

$$\mathcal{O}(\varepsilon^0): \quad \mathbf{A} \mathbf{W}_0 + \mathbf{G}_{\text{nl}}(\mathbf{W}_0) = \frac{\partial \mathbf{W}_0}{\partial \mathbf{z}} \mathbf{R}_0. \quad (\text{A } 3)$$

As the non-resonance conditions (2.9) are satisfied, one can solve for the unknown polynomial coefficients of \mathbf{W}_0 and \mathbf{R}_0 (cf. [8]). The fixed point is at the origin, therefore

$$\mathbf{w}_0^0 = 0, \quad \mathbf{r}_0^0 = 0, \quad (\text{A } 4)$$

holds.

Now, we consider the first-order terms in epsilon and the zeroth-order in \mathbf{z} in equation (A 2). At this order, no terms from the nonlinearity \mathbf{G}_{nl} arise, because it is at least quadratic in its arguments. The relevant terms at this order from the right-hand side of equation (A 2) \mathbf{W}_0 and \mathbf{R}_0 are zero (cf. equation (A 4)), while the terms from \mathbf{W}_1 and \mathbf{R}_1 remain

$$\mathcal{O}(\varepsilon, |\mathbf{z}|^0): \quad \mathbf{A} \mathbf{w}_1^0(\phi) + \mathbf{G}_{\text{ext}}(\phi) = \frac{\partial \mathbf{W}_0}{\partial \mathbf{z}} \mathbf{r}_1^0(\phi) + \frac{\partial \mathbf{w}_1^0}{\partial \phi} \Omega. \quad (\text{A } 5)$$

Setting $\mathbf{r}_1^0(\phi) = 0$, we find that the periodic solutions of (A 5) can be obtained from Dunhamel's principle as

$$\mathbf{w}_1^0 = \int_0^t e^{\mathbf{A}(t-s)} \mathbf{G}_{\text{ext}}(s) ds, \quad (\text{A } 6)$$

where we use the time evolution (2.6) of the angles. The integral in (A 6) can be evaluated numerically or solved analytically. In our setting, the external forcing can be expanded in a Fourier series leading to the expression (3.2a).

Again, the existence and smoothness properties stated by Haro & de la Llave [8] ensure the solvability of the higher-order terms in \mathbf{z} and ε in (A 2).

(b) Spectral submanifold for the near-resonant forced mechanical system

To prove theorem 3.2, we explicitly calculate $\mathbf{W}(\mathbf{z}, \phi)$ and $\mathbf{R}(\mathbf{z}, \phi)$ up to the required order of accuracy $\mathcal{O}(\mu^{2M+3})$. We first identify the relevant terms to be calculated by applying the rescaling (3.9) to the series expansion (2.14):

$$\left. \begin{aligned} \mathbf{W}(\mathbf{z}, \phi) &= \mathbf{W}_0(\mathbf{z}) + \mathcal{O}(\mathbf{z}^{2M+3}) + \varepsilon(\mathbf{w}_1^0(\phi) + \mathcal{O}(\mathbf{z})) + \mathcal{O}(\varepsilon^2) \\ &= \mathbf{W}_0(\mathbf{z}) + \mu^{2M+2} \mathbf{w}_1^0(\phi) + \mathcal{O}(\mu^{2M+3}) \\ \text{and} \quad \mathbf{R}(\mathbf{z}, \phi) &= \mathbf{R}_0(\mathbf{z}) + \mathcal{O}(\mathbf{z}^{2M+3}) + \varepsilon(\mathbf{r}_1^0(\phi) + \mathcal{O}(\mathbf{z})) + \mathcal{O}(\varepsilon^2) \\ &= \mathbf{R}_0(\mathbf{z}) + \mu^{2M+2} \mathbf{r}_1^0(\phi) + \mathcal{O}(\mu^{2M+3}). \end{aligned} \right\} \quad (\text{A } 7)$$

The first error term ($\mathcal{O}(\mathbf{z}^{2M+3})$) results from the order- $(2M+1)$ truncation of autonomous SSM (cf. equation (3.7)). The last error term arises from the truncated expansion of the SSM at the order two in ε in the expansion (2.14). The error term $\varepsilon \mathcal{O}(\mathbf{z})$ arises from the truncation of $\mathbf{W}_1(\mathbf{z}, \phi)$ at the

zeroth order in \mathbf{z} . Rewriting the invariance condition (2.14) in terms of the new variable μ , we obtain

$$\begin{aligned} & \mathbf{A}(\mathbf{W}_0(\mathbf{z}) + \mu^{2M+2} \mathbf{w}_1^0(\phi)) + \mathbf{G}_{\text{lin}}(\mathbf{W}_0(\mathbf{z})) + \mu^{2M+2} \mathbf{G}_{\text{ext}}(\phi) \\ &= \frac{\partial \mathbf{W}_0(\mathbf{z})}{\partial \mathbf{z}} \mathbf{R}_0(\mathbf{z}) + \mu^{2M+2} [\mathbf{w}_0^{(1,0)}, \mathbf{w}_0^{(0,1)}] \mathbf{R}_1(\mathbf{z}, \phi) + \mu^{2M+2} \frac{\partial \mathbf{w}_1^0(\phi)}{\partial \phi} \Omega + \mathcal{O}(\mu^{2M+3}). \end{aligned} \quad (\text{A } 8)$$

The time-varying terms in equation (A 8) are of order $\mathcal{O}(\mu^{2M+2})$. Since the autonomous dynamics $\mathbf{R}_0(\mathbf{z})$ (cf. equation (3.7)) and the corresponding $\mathbf{W}_0(\mathbf{z})$ are of lower order in μ , also the formulae from Szalai *et al.* [6], which are derived for the autonomous case, apply here. As those formulae for \mathbf{R}_0 are only applicable when the linear part of (2.4) is diagonalized, we first perform a change of coordinates $\mathbf{w}_1^0(\phi) = \mathbf{V}\mathbf{v}(\phi)$ and left-multiply (A 8) \mathbf{V}^{-1} to obtain

$$\mathcal{O}(\mu^{2M+2}): \quad \mathbf{V}^{-1} \mathbf{A} \mathbf{V} \mathbf{v} + \mathbf{V}^{-1} \begin{bmatrix} 0 \\ \mathbf{M}^{-1} \mathbf{f} \end{bmatrix} (e^{i\Omega t} + e^{-i\Omega t}) = \dot{\mathbf{v}}(\Omega t) + \begin{bmatrix} \delta_{1l} & \delta_{1(l+N)} \\ \delta_{2l} & \delta_{2(l+N)} \\ \vdots & \vdots \\ \delta_{(2N)l} & \delta_{(2N)(l+N)} \end{bmatrix} \mathbf{R}_1(\Omega t), \quad (\text{A } 9)$$

where the specific terms for $\mathbf{w}_1^{(1,0)}$ and $\mathbf{w}_1^{(0,1)}$ are taken from Szalai *et al.* [6]. The matrix $\mathbf{V}^{-1} \mathbf{A} \mathbf{V}$ is diagonal, containing the eigenvalues λ_j . Furthermore, we have also inserted the canonical forcing (3.4) in equation (A 9). For the n th coordinate equation (A 9) gives

$$\lambda_n v_n + p_n (e^{i\Omega t} + e^{-i\Omega t}) = \dot{v}_n + \delta_{nl} r_c e^{i\Omega t} + \delta_{n(l+N)} \bar{r}_c e^{-i\Omega t}, \quad (\text{A } 10)$$

where the complex amplitude p_n of the forcing is defined as

$$p_n = \mathbf{t}_n \begin{bmatrix} 0 \\ \mathbf{M}^{-1} \mathbf{f} \end{bmatrix}. \quad (\text{A } 11)$$

We observe that equation (A 10) is a linear ordinary differential equation for the unknown coefficients v_n . Therefore, the periodic solutions of (A 10) can be obtained as in the previous section from the Dunhamel's principle. Owing to the Kronecker delta in equation (A 10), three cases arise

$$v_l = \frac{p_l - r}{i\Omega - \lambda_l} e^{i\Omega t} + \frac{p_l}{-i\Omega - \lambda_l} e^{-i\Omega t}, \quad (\text{A } 12a)$$

$$v_{l+N} = \frac{\bar{p}_l}{i\Omega - \bar{\lambda}_l} e^{i\Omega t} + \frac{\bar{p}_l - \bar{r}}{-i\Omega - \bar{\lambda}_l} e^{-i\Omega t} \quad (\text{A } 12b)$$

and
$$v_n = \frac{p_n}{i\Omega - \lambda_n} e^{i\Omega t} + \frac{p_n}{-i\Omega - \lambda_n} e^{-i\Omega t}, \quad n \neq l, l+N. \quad (\text{A } 12c)$$

The amplitude p_l coincides with r (cf. equations (3.13b) and (A 11)). Therefore, the first term in (A 12a) and the second term in (A 12b) vanish. These are the terms that would create small denominators in the parametrization of the SSM (\mathbf{w}_1^0). The choice of the coefficient r_l^0 in (3.13b) eliminates these small denominators. Because we assume that the near-resonance conditions (3.8) are satisfied, small denominators in (A 12c) do not arise, unless the forcing frequency is close to the imaginary part of another eigenvalue different from λ_l and $\bar{\lambda}_l$. In this case, however, the SSM needs to be constructed tangent to this specific subspace.

Changing back from the diagonal form to the physical coordinates, we recover $\mathbf{w}_1^0(\phi)$ from (3.12a).

(c) The choice of the eigenvectors

In the following, we show that the eigenvectors \mathbf{v}_j can be formed such that the constant r_c arising in the reduced dynamics (3.13b) is purely imaginary. First, note that, for a general choice of eigenvectors, r_c is complex, i.e. can be expressed as

$$r_c = ir e^{i\varphi} = \mathbf{t}_l \begin{bmatrix} 0 \\ \mathbf{M}^{-1}\mathbf{f} \end{bmatrix} \quad (\text{A } 13)$$

and r_c is not purely imaginary for $\varphi \neq \pm n\pi$. Multiplying \mathbf{V} with $e^{i\varphi}$ and realizing that the vector \mathbf{t}_l is the l th row of \mathbf{V}^{-1} (cf. equation (3.11)), we obtain

$$e^{-i\varphi} \mathbf{t}_l \begin{bmatrix} 0 \\ \mathbf{M}^{-1}\mathbf{f} \end{bmatrix} = e^{-i\varphi} ir e^{i\varphi} = ir \quad (\text{A } 14)$$

and r_c is purely imaginary holds for $\tilde{\mathbf{V}} = e^{i\varphi} \mathbf{V}$. This proves corollary 3.6.

Following the proof of corollary 3.6, we show that, in case of purely symmetric system matrices ($\mathbf{N} = \mathbf{0}$ and $\mathbf{G} = \mathbf{0}$) and structural damping, the constant r_c is purely imaginary if we mass normalize the mode shapes \mathbf{e}_j . With the real mode shape matrix \mathbf{E} and the notation (2.5), the matrix of eigenvectors \mathbf{V} is given by

$$\mathbf{V} = \begin{bmatrix} \mathbf{E} & \mathbf{E} \\ \mathbf{E}\mathbf{\Lambda} & \mathbf{E}\tilde{\mathbf{\Lambda}} \end{bmatrix}. \quad (\text{A } 15)$$

To compute the constant r_c explicitly, we need to compute the inverse of the matrix \mathbf{V} (cf. equation (3.13b)). By clockwise inversion of (A 15), we obtain

$$\mathbf{V}^{-1} = \begin{bmatrix} \mathbf{E}^{-1} + (\tilde{\mathbf{\Lambda}} - \mathbf{\Lambda})^{-1} \mathbf{E}^{-1} \mathbf{\Lambda} \mathbf{E}^{-1} & -(\tilde{\mathbf{\Lambda}} - \mathbf{\Lambda})^{-1} \mathbf{E}^{-1} \\ (\tilde{\mathbf{\Lambda}} - \mathbf{\Lambda})^{-1} \mathbf{E}^{-1} \mathbf{\Lambda} \mathbf{E}^{-1} & (\tilde{\mathbf{\Lambda}} - \mathbf{\Lambda})^{-1} \mathbf{E}^{-1} \end{bmatrix}. \quad (\text{A } 16)$$

As the mode-shape matrix \mathbf{E} and its inverse are real, the last N columns of (A 16) are purely imaginary. Therefore, a multiplication by the forcing in equation (3.13b) will always lead to a purely imaginary r_c .

(d) Amplitude, phase shift and stability of the T -periodic orbits of the reduced dynamics

In the following, we compute periodic orbits with the same period as the forcing of the reduced dynamics (3.13b). These orbits will determine the steady-state response of the system (2.1). First, we transform the reduced dynamics (3.12b) into the polar coordinates (3.16), which yields

$$\left. \begin{aligned} \dot{\rho} &= \text{Re}(\lambda_l) \rho + \sum_{m=1}^M \text{Re}(\beta_m) \rho^{2m+1} + \varepsilon r \sin(\theta - \phi), \\ \dot{\theta} &= \text{Im}(\lambda_l) + \sum_{m=1}^M \text{Im}(\beta_m) \rho^{2m} + \frac{\varepsilon}{\rho} (r \cos(\theta - \phi)) \\ \text{and} \quad \dot{\phi} &= \Omega. \end{aligned} \right\} \quad (\text{A } 17)$$

With the change of coordinates $\psi = \theta - \phi$, the dynamics (A 17) can be rewritten as

$$\dot{\rho} = \text{Re}(\lambda_l) \rho + \sum_{m=1}^M \text{Re}(\beta_m) \rho^{2m+1} + \varepsilon r \sin(\psi) = a(\rho) + \varepsilon r \sin(\psi), \quad (\text{A } 18)$$

$$\dot{\psi} = \text{Im}(\lambda_l) + \sum_{m=1}^M \text{Im}(\beta_m) \rho^{2m} + \frac{\varepsilon}{\rho} (r \cos(\psi)) - \Omega = b(\rho) + \frac{\varepsilon}{\rho} (r \cos(\psi)) - \Omega \quad (\text{A } 19)$$

$$\text{and} \quad \dot{\phi} = \Omega. \quad (\text{A } 20)$$

The angle ψ represents the phase shift between the forcing and the system response. At the steady state of (2.4), the amplitude ρ , as well as the phase shift ψ are constant. The trigonometric functions in (A 18) and (A 19) can be eliminated by solving (A 18) for $\sin(\psi)$ and (A 19) for $\cos(\psi)$ and adding the square of both equations. Thereby we obtain equation (3.18). We determine the phase relation (3.19) by solving the steady-state response of equation (A 19) for ψ . The stability of such solutions can be obtained by evaluating the eigenvalues of the Jacobian of (A 18) and (A 19) with respect to ρ and ψ , which we state in (3.20).

Appendix B. Coefficients for the autonomous spectral submanifold and the reduced dynamics

We recall here for completeness the parametrization of the autonomous SSM ($\mathbf{W}_0(\mathbf{z})$) and the reduced dynamics ($\mathbf{R}_0(\mathbf{z})$) from Szalai *et al.* [6]. To diagonalize the linear part, we apply the transformation

$$\mathbf{y} = \mathbf{V}\mathbf{x} \quad (\text{B } 1)$$

to the autonomous limit ($\varepsilon \rightarrow 0$) of system (2.4) and obtain

$$\dot{\mathbf{y}} = \mathbf{V}^{-1}\mathbf{A}\mathbf{V}\mathbf{y} + \mathbf{V}^{-1}\mathbf{G}_{\text{nl}}(\mathbf{V}\mathbf{y}) = \mathbf{A}\mathbf{y} + \mathbf{G}(\mathbf{y}). \quad (\text{B } 2)$$

The Taylor series of the j th entry of nonlinear terms \mathbf{G} is

$$\mathbf{G}_j = \sum_{\mathbf{m} \in \mathbb{N}_0^{2N}} g_j^{\mathbf{m}} \mathbf{y}^{\mathbf{m}}. \quad (\text{B } 3)$$

As Szalai *et al.* [6], we use $(p@j)$ to denote an integer multi-index whose elements are zero, except for the index at the j th position, which is equal to p , i.e.

$$(p@j) := (0, \dots, 0, p, 0, \dots, 0) \in \mathbb{N}^{2N}. \quad (\text{B } 4)$$

We also use this notation to refer to multi-indices with multiple entries $(p@j_1, q@j_2)$ and in case of $j_1 = j_2$ the corresponding entry is $p + q$, i.e.

$$(p@j_1, q@j_2) := (0, \dots, 0, p, 0, \dots, 0, q, 0, \dots, 0),$$

$$(p@j, q@j) := (0, \dots, 0, p + q, 0, \dots, 0).$$

With this notation the coefficients of the parametrization $\mathbf{W}_0(\mathbf{z})$ for $j = 1, \dots, 2N$ are given by

$$w_j^{(1,0)} = \delta_{j\bar{l}}, \quad w_j^{(1,0)} = \delta_{j(l+N)},$$

$$w_j^{(2,0)} = \frac{g_j^{(2@l)}}{2\lambda_l - \lambda_j}, \quad w_j^{(1,1)} = \frac{g_j^{(1@l,1@l+N)}}{\lambda_l + \bar{\lambda}_l - \lambda_j}, \quad w_j^{(0,2)} = \frac{g_j^{(2@(l+N))}}{2\bar{\lambda}_l - \lambda_j},$$

$$w_j^{(3,0)} = \frac{\sum_{q=1}^{2N} (1 + \delta_{lq}) g_j^{(1@l,1@q)} w_q^{(2,0)} + g_j^{(3@l)}}{3\lambda_l - \lambda_j},$$

$$w_j^{(0,3)} = \frac{\sum_{q=1}^{2N} (1 + \delta_{(l+N)q}) g_j^{(1@(l+N),1@q)} w_q^{(0,2)} + g_j^{(3@(l+N))}}{3\bar{\lambda}_l - \lambda_j},$$

$$w_j^{(2,1)} = (1 - \delta_{j\bar{l}}) \frac{\sum_{q=1}^{2N} (1 + \delta_{lq}) g_j^{(1@l,1@q)} w_q^{(1,1)} + \sum_{q=1}^{2N} (1 + \delta_{(l+N)q}) g_j^{(1@(l+N),1@q)} w_q^{(2,0)} + g_j^{(3@l)}}{2\lambda_l + \bar{\lambda}_l - \lambda_j}$$

and

$$w_j^{(1,2)} = (1 - \delta_{j(i+N)}) \frac{\sum_{q=1}^{2N} (1 + \delta_{lq}) g_j^{(1@l,1@q)} w_q^{(0,2)} + \sum_{q=1}^{2N} (1 + \delta_{(l+N)q}) g_j^{(1@(l+N),1@q)} w_q^{(1,1)} + g_j^{(2@l,1@(i+N))}}{\lambda_l + 2\bar{\lambda}_l - \lambda_j}.$$

The coefficient β_1 of the reduce dynamics (3.7) is given by

$$\beta_1 = \sum_{q=1}^{2N} (1 + \delta_{lq}) g_j^{(1@l,1@q)} w_q^{(1,1)} + \sum_{q=1}^{2N} (1 + \delta_{(l+N)q}) g_j^{(1@(l+N),1@q)} w_q^{(2,0)} + g_l^{(2@l,1@(l+N))}. \quad (\text{B } 5)$$

To compute the $\mathcal{O}(5)$ autonomous SSM ($M=2$), we provide a Matlab script as the electronic supplementary material.

References

- Rosenberg R. 1966 On nonlinear vibrations of systems with many degrees of freedom. *Adv. Appl. Mech.* **9**, 155–242. (doi:10.1016/S0065-2156(08)70008-5)
- Shaw S, Pierre C. 1993 Normal modes for non-linear vibratory systems. *J. Sound. Vib.* **164**, 85–124. (doi:10.1006/jsvi.1993.1198)
- Haller G, Ponsioen S. 2016 Nonlinear normal modes and spectral submanifolds: existence, uniqueness and use in model reduction. *Nonlinear. Dyn.* **86**, 1493–1534. (doi:10.1007/s11071-016-2974-z)
- Neild S, Champneys A, Wagg D, Hill T, Cammarano A. 2015 The use of normal forms for analysing nonlinear mechanical vibrations. *Phil. Trans. R. Soc. A* **373**, 20140404. (doi:10.1098/rsta.2014.0404)
- Jain S, Tiso P, Haller G. 2017 Exact nonlinear model reduction for a von Kármán beam: slow-fast decomposition and spectral submanifolds. *J. Sound Vib.* **423**, 195–211. (doi:10.1016/j.jsv.2018.01.049)
- Szalai R, Ehrhardt D, Haller G. 2017 Nonlinear model identification and spectral submanifolds for multi-degree-of-freedom mechanical vibrations. *Proc. R. Soc. A* **473**, 20160759. (doi:10.1098/rspa.2016.0759)
- Ponsioen S, Pedergrana T, Haller G. 2018 Automated computation of autonomous spectral submanifolds in nonlinear modal analysis. *J. Sound Vib.* **420**, 269–295. (doi:10.1016/j.jsv.2018.01.048)
- Haro A, de la Llave R. 2006 A parameterization method for the computation of invariant tori and their whiskers in quasi-periodic maps: rigorous results. *J. Differ. Equ.* **228**, 530–579. (doi:10.1016/j.jde.2005.10.005)
- Jiang D, Pierre C, Shaw S. 2005 Nonlinear normal modes for vibratory systems under harmonic excitation. *J. Sound Vib.* **288**, 791–812. (doi:10.1016/j.jsv.2005.01.009)
- Sinha S, Redkar S, Butcher E. 2005 Order reduction of nonlinear systems with time periodic coefficients using invariant manifolds. *J. Sound. Vib.* **284**, 985–1002. (doi:10.1016/j.jsv.2004.07.027)
- Gabale A, Sinha S. 2011 Model reduction of nonlinear systems with external periodic excitations via construction of invariant manifolds. *J. Sound. Vib.* **330**, 2596–2607. (doi:10.1016/j.jsv.2010.12.013)
- Guckenheimer J, Holmes P. 2002 *Nonlinear oscillations, dynamical systems, and bifurcations of vector fields*. Applied Mathematical Sciences, vol. 42. New York, NY: Springer Science+Business Medis. (corr. 7. printing edition).
- Jezequel L, Lamarque C. 1991 Analysis of non-linear dynamical systems by the normal form theory. *J. Sound. Vib.* **149**, 429–459. (doi:10.1016/0022-460X(91)90446-Q)
- Neild S, Wagg D. 2011 Applying the method of normal forms to second-order nonlinear vibration problems. *Proc. R. Soc. A* **467**, 1141–1163. (doi:10.1098/rspa.2010.0270)
- Touzé C, Amabili M. 2006 Nonlinear normal modes for damped geometrically nonlinear systems: application to reduced-order modelling of harmonically forced structures. *J. Sound Vib.* **298**, 958–981. (doi:10.1016/j.jsv.2006.06.032)
- Nayfeh A, Mook D. 1995 *Nonlinear oscillations*. New York, NY: Wiley.
- Cveticanin L, Zukovic M, Balthazar JM. 2017 *Dynamics of mechanical systems with non-ideal excitation*. Berlin, Germany: Springer.
- Peeters M, Kerschen G, Golinval JC. 2011 Dynamic testing of nonlinear vibrating structures using nonlinear normal modes. *J. Sound Vib.* **330**, 486–509. (doi:10.1016/j.jsv.2010.08.028)
- Klotter K. 1953 Steady-state vibrations in systems having arbitrary restoring and arbitrary damping forces. In *Proc. Symp. on Nonlinear Circuit Analysis, New York, NY, 23, 24 April*, pp. 234–257. Brooklyn, NY: Polytechnic Institute of Brooklyn, Microwave Research Institute.

20. Rosenberg R, Atkinson C. 1959 On the natural modes and their stability in nonlinear two-degree-of-freedom systems. *J. Appl. Mech.* **26**, 377–385.
21. Hill T, Cammarano A, Neild S, Wagg D. 2015 Interpreting the forced responses of a two-degree-of-freedom nonlinear oscillator using backbone curves. *J. Sound Vib.* **349**, 276–288. (doi:10.1016/j.jsv.2015.03.030)
22. Hill TL, Cammarano A, Neild SA, Barton DAW. 2017 Identifying the significance of nonlinear normal modes. *Proc. R. Soc. A* **473**, 20160789. (doi:10.1098/rspa.2016.0789)
23. Kerschen G, Peeters M, Golinval J, Vakakis A. 2009 Nonlinear normal modes, Part I: a useful framework for the structural dynamicist. *Mech. Syst. Signal Process.* **23**, 170–194. Special Issue: Non-linear Structural Dynamics. (doi:10.1016/j.ymsp.2008.04.002)
24. Cabré X, Fontich E, de la Llave R. 2003 The parameterization method for invariant manifolds I: manifolds associated to non-resonant subspaces. *Indiana Univ. Math. J.* **52**, 283–328. (doi:10.1512/iumj.2003.52.2245)
25. Kelley A. 1969 Analytic two-dimensional subcenter manifolds for systems with an integral. *Pacific J. Math.* **29**, 335–350. (doi:10.2140/pjm.1969.29.335)
26. Wagg D, Neild S. 2014 *Nonlinear vibration with control: for flexible and adaptive structures*. Solid Mechanics and its Applications, 2nd edition, vol. 218. Berlin, Germany: Springer.
27. Kerschen G. 2014 *Modal analysis of nonlinear mechanical systems*. Vienna, Austria: CISM International Centre for Mechanical Sciences, Springer.
28. Dhooge A, Govaerts W, Kuznetsov Y. 2003 MATCONT: a MATLAB package for numerical bifurcation analysis of ODEs. *ACM Trans. Math. Softw.* **29**, 141–164. (doi:10.1145/779359.779362)
29. Neild S, Wagg D. 2013 A generalized frequency detuning method for multidegree-of-freedom oscillators with nonlinear stiffness. *Nonlinear Dyn.* **73**, 649–663. (doi:10.1007/s11071-013-0818-7)
30. Touzé C, Thomas O, Chaigne A. 2004 Hardening/softening behaviour in non-linear oscillations of structural systems using non-linear normal modes. *J. Sound Vib.* **273**, 77–101. (doi:10.1016/j.jsv.2003.04.005)